

See discussions, stats, and author profiles for this publication at: <https://www.researchgate.net/publication/279313394>

Spectral Wave Conditions in the Colombian Pacific Ocean

Article in *Ocean Modelling* · June 2015

DOI: 10.1016/j.ocemod.2015.06.005

CITATIONS

5

READS

281

4 authors, including:



Jesus Portilla-Yandun

Escuela Politécnica Nacional

29 PUBLICATIONS 250 CITATIONS

[SEE PROFILE](#)



Roberto Padilla-Hernandez

National Oceanic and Atmospheric Administration

28 PUBLICATIONS 365 CITATIONS

[SEE PROFILE](#)



Luigi Cavalieri

Italian National Research Council

215 PUBLICATIONS 5,991 CITATIONS

[SEE PROFILE](#)

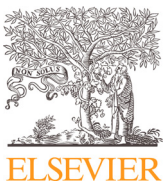
Some of the authors of this publication are also working on these related projects:



WASS: Wave Acquisition Stereo System [View project](#)



GLOWAC [View project](#)



Spectral wave conditions in the Colombian Pacific Ocean



Jesús Portilla^{a,b,*}, Ana Lucía Caicedo^c, Roberto Padilla-Hernández^d, Luigi Cavaleri^e

^a Universidad San Francisco de Quito (USFQ), Av. Diego de Robles y Vía Interoceánica, Quito, Ecuador

^b Escuela Politécnica Nacional, Ladrón de Guevara E11-253, Quito, Ecuador

^c Dirección General Marítima de Colombia, Centro de Investigaciones Oceanográficas e Hidrográficas del Pacífico (DIMAR-CCCP), Vía El Morro, Capitanía de Puerto San Andrés de Tumaco, Nariño, Colombia

^d National Oceanic and Atmospheric Administration, IMSG at NOAA/EMC/NCEP/MMAB, NOAA Center for Weather and Climate Prediction, 5380 University Research Court, College Park, MD 20740, USA

^e Istituto di Scienze Marine, Consiglio Nazionale delle Ricerche (ISMAR-CNR), Arsenale – Tesa 104, Castello 2737/F, 30122, Venice, Italy

ARTICLE INFO

Article history:

Received 3 July 2014

Revised 4 June 2015

Accepted 17 June 2015

Available online 24 June 2015

Keywords:

Colombian Pacific Ocean

Spectral wave climate

Triaxys buoy

ECMWF

ERA-Interim

Spectral partitioning

ABSTRACT

A comprehensive characterization of the wave conditions in the Colombian Pacific based on wave spectra is presented. The spectral approach offers a detailed description of the different wave regimes, their associated meteorological conditions and their variation in time and geographical space. To this end, two complementary data sources are used, the first is representative for the near-shore zone and comes from observations of the local monitoring network. The second comes from numerical wave model results that cover the open ocean. The measured data used are the first systematically collected spectral wave data in the Eastern Equatorial Pacific. Modelled spectra correspond to the ERA-Interim database of the European Centre for Medium-Range Weather Forecasts that spans 35 years. An indicator for statistical analysis of the wave spectra has been introduced which basically consists of the occurrence probability of spectral partitions. This indicator has proved to be skilful for the task of defining spectral wave systems of both model and, the more challenging, measured spectra. Following the spectral approach and using this new indicator, six main wave regimes are found in the study area. Two of these systems have well defined swell characteristics that are originated outside the study area in the northern and southern hemispheres. Other three wave systems are to a certain extent associated to the local winds, and in general may be classified as old wind-seas. These are found to flow northeastwards, westwards, and southwards. The sixth system is composed of locally generated wind waves of relatively low magnitude that propagate in several directions. The time variability of these wave systems is highly dependent on the boreal and austral winter storms and on the tropical conditions, in such a way that the wave energy propagation to the region is rather constant along the year, but their origin and characteristics vary significantly.

© 2015 Elsevier Ltd. All rights reserved.

1. Introduction

The focus of the present study is the characterization of the wave conditions in the Colombian Pacific Zone using spectral wave data from both *in-situ* measurements and numerical model results. The spectral approach needs to be emphasized because wave conditions in the study area are rather complex due to the presence of swells arriving from different parts of the Pacific Ocean. Under these conditions, integral wave parameters like significant wave height, mean wave period, and mean wave direction (H_{m0} , $T_{m-1,0}$, θ_m , see Appendix A for definitions) poorly describe the complexity of the wave field because they correspond to vectorial means. On the contrary for many applications like climate assessment, navigation,

structural design, among others, it is more important to know which (two or more) wave systems are involved, and what are their specific characteristics, rather than having an averaged value (e.g., WMO, 1998). The wave spectrum is the most standard approach to statistically describe the wave conditions, and that is typically derived from the measured data of modern instrumentation and directly from numerical spectral models (e.g., Holthuijsen, 2007). In the spectral approach, the complexity of the sea surface is represented as the superposition of a finite number of harmonic components of different frequencies and directions (i.e., Fourier representation). This representation gives a complete description of the sea surface in a stochastic sense (Barber and Ursell, 1948; Deacon, 1949; Ochi, 2005).

The Colombian Pacific area is under the influence of the InterTropical Convergence Zone (ITCZ), a global scale phenomenon that encircles the Earth along the tropics. The ITCZ is where the northerly and southerly trade winds converge (with respectively southwest-erly and northwesterly predominant flow directions). Because of this,

* Corresponding author. Tel.: +593 998040979; fax: +593 22890070.
E-mail address: jportilla@ymail.com, jportilla@usfq.edu.ec (J. Portilla).

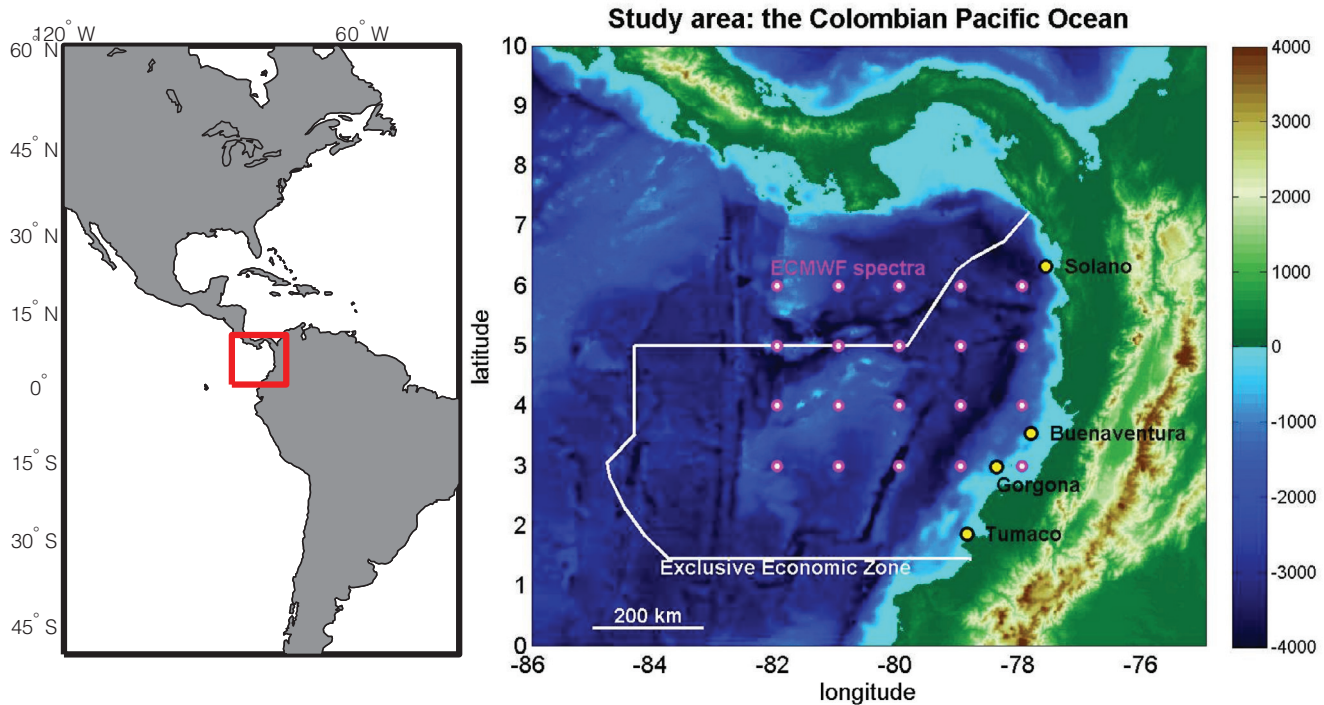


Fig. 1. The Colombian Pacific. Orography and bathymetry data from Smith and Sandwell (1997). The vertical colour bar scale indicates metres. The Exclusive Economic Zone limits are indicated in white (data from marineregions.org, 2014). The ECMWF spectral output points, and the DIMAR moorings are shown in magenta and yellow respectively. (For interpretation of the references to colour in this figure legend, the reader is referred to the web version of this article.)

mean wind speeds in the ITCZ are typically low with the presence of seasonal and specific events of moderate magnitudes (e.g., Raymond et al., 2006). In addition, the boreal and austral winter activities influence the latitude of the ITCZ location, and these variations drive the meteorological conditions of the region (e.g., Barry and Chorley, 2009). Apart from the ITCZ, other interesting meteorological phenomena in the area are the wind jets flowing through the mountain passes of Central America. These derive from the large pressure gradients between the northern cooler atmospheric masses of North America and the Caribbean region and the warmer air masses of the Pacific. These are the so called Tehuantepec, Papagayo, and Panama wind jets (e.g., Chelton et al., 2000a, 2000b; Schultz et al., 1998). The dynamics of both the ITCZ and the wind jets of Central America generate to a large extent the local wind waves. However, the main source of wave energy is due to swells originated outside the area, especially in the extratropical storm belt of the southern hemisphere. These swell sources can be traced back to areas as remote as the Antarctic region (e.g., Alves, 2006; Collard et al., 2009; Portilla, 2012; Semedo et al., 2013).

Two main wave data sources constitute the basis to characterize the wave conditions in the Colombian Pacific. The first are observations from a local monitoring network owned by DIMAR (*Dirección General Marítima de Colombia*) composed of four directional Triaxys buoys arranged along the Colombian Pacific coast moored at depths of about 130 m. This network has been operational since 2009, with several gaps due to failure or maintenance (CIOH, 2014). The second data source corresponds to numerical results from the WAM wave model operated by the European Centre for Medium-Range Weather Forecasts (ECMWF, Reading, UK). This data source consists of time series of directional wave spectra from 1979 to 2013 (Dee et al., 2011). From the computational grid of WAM, twenty locations within the study area have been used (see Fig. 1). The purpose of combining these two data sources for the analysis is to provide an overall view of the wave characteristics using the best information available at

present, quality controlled observations in the near-shore zone and validated model results in the open ocean. Other data consisting of model gridded integral parameters are also incorporated into the analysis. Details of the overall database are given in Section 2.

Naturally each data source has advantages and disadvantages. For instance, measuring buoys are specifically placed for serving coastal applications and therefore they are located rather close to the coast. Nevertheless the moorings are in sufficiently deep water in this case so that the swell characteristics are not significantly influenced by bathymetry and can be assessed rather neatly. However, depending on the specific location, buoys can be sheltered from certain incoming wave directions. This affects the long-term wave characteristics at the study site. Specifically the buoys located in the northern part of the considered area are partially sheltered from waves coming from the North Pacific (see Fig. 1), but are directly exposed to waves coming from the South Pacific. The reverse is true for the buoys located in the southern part. In addition, data discontinuity is almost impossible to avoid in observations and that is always an inconvenience. Other disadvantages of measured data are possible measurement errors, which are dealt with here using a dedicated quality control procedure. Finally, buoys are location specific, so they provide information at one point only, contrarily to the modelled data which provide detailed spatial and temporal information. The two data sources, modelled and measured ones, are thus to a large extent complementary. However, we stress that a comparison is not intended here, because the two data sources are not directly comparable. The main reason is that the model data from ECMWF correspond to a global grid implementation which is not designed to resolve near-shore processes. Therefore, any comparison can only be done qualitatively and the main purpose here is to use the two sources to provide on the whole the best comprehensive picture of the local wave climate presently possible.

Although at present the wave spectrum is the standard variable for wave representation, the methods for describing it statistically

are currently not standard. In most cases, wave characterizations are based on integral parameters, like significant wave height and mean wave period. Often trivariate plots of these variables plus energy or their bivariate probability functions can be very illustrative (for instance in wave energy and coastal engineering applications, e.g., [EPRI, 2011](#)). Besides statistics of mean direction are also commonly included, for instance in the form of wave roses. However, the main disadvantage of using integral parameters is that a large portion of the detailed information contained in the wave spectrum is blurred or lost. This issue is especially critical in locations where two or more different wave systems coexist, because in these cases integral parameters do not accurately represent the wave conditions. The main purpose of the present methodology is to obtain spectral wave statistics while preserving the details of the spectrum. To this end, a combination of indicators for the 2D and 1D spectra are used. For an overall view, integral parameters are also included. It turns out that the spectral parameters can help identifying the different wave regimes that characterize the local wave climate. Especially the occurrence probability of spectral partitions, computed from the 2D spectra, has proved skilful, not only to elucidate the different wave regimes, but also to define quantitatively the energy distribution in the spectral domains. Other parameters like the average energy spectra and average integral parameters have also been useful to assess the energy content and variability of the different wave regimes. This methodology is presented in [Section 3](#).

The results of this analysis, for buoy and model spectra, turn out to be enlightening in showing the complexity of the wave conditions at the edges of a large ocean, in this case the Colombian coast of the Pacific Ocean. Here we find both the effects of the long distance propagating swells and of the waves generated by the local, often orographically driven, wind systems. The results for the two different sources are reported respectively in [Section 4](#) (buoys) and [Section 5](#) (model). A short summary of the general findings is given in [Section 6](#).

2. Study area and data sources

2.1. Study area

The Colombian Pacific Zone is located in South America, between $1^{\circ}26'N$ and $7^{\circ}13'N$ in latitude and $77^{\circ}W$ and $85^{\circ}W$ in longitude ([Fig. 1](#)). It is therefore characterized by tropical meteorological conditions. Concerning the configuration of the oceanic basin, it is worth noticing the narrow continental shelf, especially near Solano bay, with dimensions in the order of a few tens of kilometres. Beyond this margin a narrow slope zone is observed, directly followed by the deep ocean. Another important geographical characteristic is that the whole area has the configuration of a large bay being surrounded at the north by Central America and at the southeast by some peninsulas of South America. Because of this, northerly and southerly waves can be partially blocked.

2.2. Buoy data

Directional wave spectra in the study area have been measured systematically since 2009 by a network of Triaxys buoys. This is a spherical buoy 1.10 m in diameter ([Shih, 2003; Skey and Miles, 1999](#)) with three accelerometers disposed orthogonally (in the x , y , and z axes), three rate gyros, and a reference compass. The sensors provide information about the heave, pitch, and roll motions by means of standard Fourier analysis techniques (e.g., [Kuik et al., 1988; Benoit et al., 1997](#)), and the full 2D spectrum is estimated according to the Maximum Entropy Method, MEM ([Nwogu, 1989](#)). The buoys are moored near the edge of the continental shelf at Tumaco, Gorgona, Buenaventura, and Solano locations (see [Fig. 1](#)). The measured spectrum has 129 frequencies, from 0.0 to 0.64 Hz at regular intervals of 0.005 Hz, and 120 directions, from 0° to 360° also at regular intervals of 3° . The sample interval is 2 Hz, the length of the record is

Table 1
Monitoring buoy locations.

Station	Longitude	Latitude	Mooring water depth
Solano Bay	$77^{\circ}30'39.6''W$	$6^{\circ}15'28.6''N$	130 m
Buenaventura	$77^{\circ}43'47.71''W$	$3^{\circ}32'0.87''N$	150 m
Gorgona island	$78^{\circ}15'57.24''W$	$2^{\circ}58'3.41''N$	135 m
Tumaco	$78^{\circ}52'55.11''W$	$1^{\circ}54'14.19''N$	146 m

Table 2
Number of 2D wave spectra from buoy observations.

	Tumaco	Gorgona	Buenaventura	Solano
January	743	–	744	–
February	863	37	245	–
March	350	–	734	–
April	351	–	350	–
May	28	19	39	–
June	33	58	1440	449
July	1169	923	1196	22
August	1487	1390	79	–
September	1483	719	718	–
October	451	40	743	–
November	199	–	720	–
December	1342	–	744	–
Total	8499	3186	7752	471

30 min and the records are hourly. The overall time span of the measurements goes from 2009 to 2013 with the mentioned data gaps due to buoy failure or maintenance. Quality control has been applied to the data with a dedicated algorithm (see [Portilla et al., 2013](#) for details). The location and water depth of the moorings are listed in [Table 1](#), and [Table 2](#) gives an overview of the amount of spectral data available for the analysis.

2.3. ECMWF modelled data

International centres like ECMWF or NOAA-NCEP run different numerical meteorological, ocean and wave models on global and regional scales, archiving many environmental variables. For waves the ECMWF operational model is WAM Cycle IV ([Komen et al., 1994; Janssen, 2008](#)), an evolution of the prototype third-generation spectral wave models. Its latest version includes a modified wind input term ([Janssen, 1991, 2004](#)), and a reformulation of the dissipation by white-capping ([Bidlot et al., 2007](#)). These new expressions account for the effect of the wave field on the atmospheric forcing through the roughness length parameter allowing for a two way coupling with the atmospheric model. WAM solves the wave energy balance [Eq. \(1\)](#) defined in geographical, spectral and time domains.

$$\frac{\partial F}{\partial t} + \frac{\partial}{\partial x}(c_x F) + \frac{\partial}{\partial y}(c_y F) + \frac{\partial}{\partial \theta}(c_\theta F) + \frac{\partial}{\partial \sigma}(c_\sigma F) = S_{in} + S_{nl} + S_{wc} + S_{bf} \quad (1)$$

The left hand side of this equation accounts for wave energy advection, where: $F = F(\sigma, \theta, x, y, t)$ represents the wave spectrum, x and y are the space coordinates, t is time, θ is the wave direction, σ is the relative frequency, c_x and c_y represent the propagation velocities in geographical space, and c_θ and c_σ are the propagation velocities in spectral space which account for shoaling and refraction. The right hand side of the equation accounts for energy sources (energy transfer by wind, S_{in}), sinks (energy dissipation by white-capping, S_{wc} and bottom friction, S_{bf}) and non-linear energy transfer (quadruplets interactions, S_{nl}). The wave model spectrum is discretized in 24 directions ranging from 7.5° to 352.5° in regular steps of 15° . Frequency is discretized in 30 bins ranging from 0.0345 to 0.5476 Hz in geometric sequence (see [ECMWF, 2011](#) for details). The model is implemented on a global coverage 110 km uniform resolution grid.

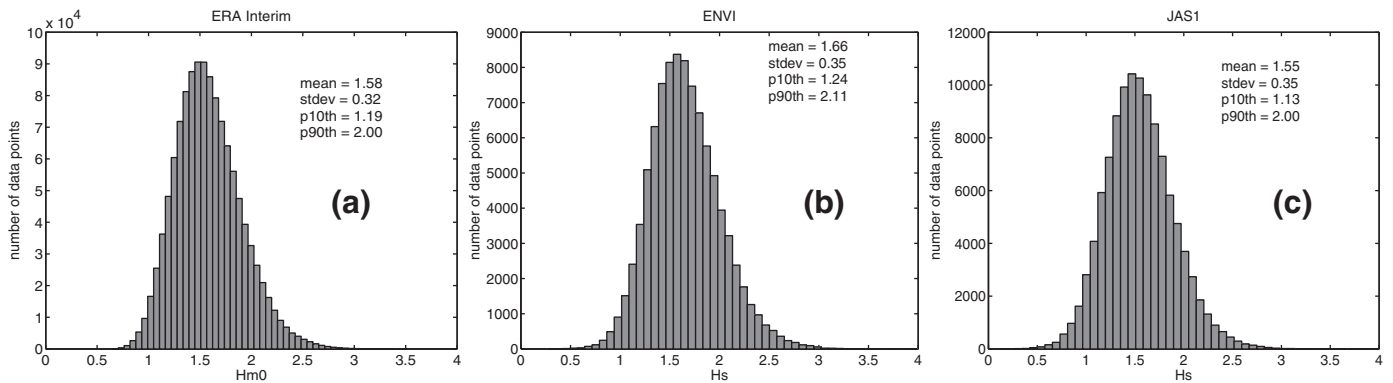


Fig. 2. Histograms of significant wave height for (a) ERA-Interim (1989–2001), (b) EnviSat (2002–2009), and (c) Jason (2002–2009).

The ECMWF data used in the present study correspond to the ERA-Interim archive (Dee et al., 2011), a reanalysis project that covers the period from 1979 to the present. There are some characteristics that make the ERA-Interim archive unique. First, these data have been extensively evaluated and verified (e.g., Dee et al., 2011; Tavolato and Isaksen, 2011; Aarnes et al., 2015; also Bidlot and Abdalla, 2015, personal communication) and therefore as far as historical model data are concerned this is one of the most reliable existing database. The overall performance of the ERA-Interim data reported for H_{m0} corresponds to a RMSE value of about 40 cm, a negative bias of about 12 cm, scatter index in the order of 17%, and R^2 higher than 0.95 (www.ecmwf.int, Bidlot and Abdalla, personal communication). It should be noted however that the data on which these validations are based come from buoy observations located mainly in the northern hemisphere because of the better monitoring coverage. In general the performance of global models is lower in the equatorial zone because of the greater challenge in representing remotely generated swells (see for instance the results obtained by Ardhuin et al., 2010). Second, the ECMWF dataset is very comprehensive for the available results. As for waves, the ERA-Interim archive contains many integral wave parameters including significant wave height (H_{m0}), mean wave period ($T_{m-1,0}$), and mean wave direction (θ_m), relevant for the present analysis. Furthermore, the most important product for the present approach is the availability of directional spectra, archived for every point of the computational grid and for the whole reanalysis period with 6 h output interval. This allows undertaking detailed analyses, as the one presented here, by identifying the spectral wave components and elucidating relevant aspects of the local wave climate. These include the dominant wave systems, their frequency and direction domains, possible genesis and generation zone, among other characteristics.

2.4. Data quality and limitations

A general issue, when dealing with different data sources, is their compatibility. In particular, the discretization of the wave spectrum is commonly problematic. Note that the $f\text{-}\theta$ discretization is different in the two data sources considered. They do not only differ in the cut-off frequency limits, but also in their frequency increments. Numerical models typically use a geometric sequence for this increment, which is convenient from the numerical point of view and a good way to optimize computational costs. On the contrary, the frequency interval of buoy measurements is generally constant because they are produced by processing the observed signal (accelerations in the case of buoys) using Fourier analysis (sometimes a different interval is reported for swell and wind sea). These differences are particularly troublesome when spectra from different sources need to be matched, for instance for model comparison and evaluation. However, this issue is not critical here because, as already mentioned, our

purpose is to use the available information in a fully complementary way, taking into account both the advantages and limitations of the two sources. A possibly more crucial aspect is that, contrary to model 2D spectra, the wave spectra derived from buoy measurements are only an estimate based on the first four Fourier parameters a_1 , a_2 , b_1 , b_2 of the directional distribution at each frequency (see Longuet-Higgins et al., 1963, and Kuik et al., 1988). Therefore, whichever the method used for evaluating the distributions, the buoy spectra are always smoothed approximations of the true sea state. This is particularly important when we have two or more wave systems advecting energy within the same frequency range, but with different directions.

While we focus our analysis on the wave spectra and the related statistics, it is of course of interest to be aware of the accuracy of the model data we want to analyse. The ERA-Interim results have been amply validated and the related statistics have been reported by Dee et al. (2011) and are available at the ECMWF website (www.ecmwf.int).

More specifically, focusing on the area of our present interest, Fig. 2 shows the histograms of significant wave height and some of their metrics compared to two satellite missions EnviSat and Jason. It can be seen that there is a negative bias (of about -8 cm) of ERA compared to EnviSat, while this bias is positive (+3 cm) compared to Jason. The other metrics like the standard deviation and 10th and 90th percentiles are also in good agreement, and in the order of the official statistics presented by ECMWF and in particular by the cited Bidlot and Abdalla. Note that significant wave height is compared here for different periods of time so that the comparison is statistically independent. Note that, although there is an overlapping period between ERA and the two missions, a time matching comparison (scatter plot) is not possible since ERA has assimilated part of those satellite data, so that any comparison would not be statistically independent. Nevertheless, such a comparison (not shown here) gives the same level of agreement of Fig. 2. Note also that a parallel comparison with buoy data is not directly possible because the buoy data are affected by the coastal geometry, and this is only crudely represented in the coarse ERA grid. Besides the same ERA grid resolution is not compatible with the limited distance of the buoys from the coast. In any case comparisons as the ones in Fig. 2 reassure about the good quality of the model data we are going to use for our analysis.

It is worth mentioning that recent developments concerning the basic processes of wave evolution (e.g., Cavalieri et al., 2007; Ardhuin et al., 2010; Babanin 2011) have resulted in new parameterizations integrated into the state-of-the-art numerical models (see the WAVEWATCH III model as described by Tolman et al., 2013, and Tolman, 2014, and the WAM model as reported in www.ecmwf.int). In this regard, one of the objectives of the present characterization is to lay the groundwork for the modelling framework presently being implemented by DIMAR. This information is crucial to understand the

relevant processes at play and for undertaking any action in regard to model calibration and validation.

3. Analysis approach

3.1. Spectral variables

The description and characterisation of waves is in general carried out using integral parameters like significant wave height, mean wave period, and mean propagation direction. This approach is acceptable when the wave conditions are not complex from the spectral point of view, for instance in places where wind forcing dominates the local climate. However, these conditions are hardly found in nature, even less so in the open ocean. Specifically the Colombian Pacific Coast is exposed to swells propagating from the Northern and Southern Pacific Ocean, and having two or more wave systems with completely different origin is the general rule. The magnitude of these wave systems is moderate on average, but specific events can be very harsh, including also locally generated waves. Under these conditions the spectral details can be important for several applications like climate studies, sediment transport, coastal engineering, and navigation, among others. Although at present several techniques have been developed to extract information from wave spectra (namely in the field of data mining and clustering algorithms, e.g., Boukhanovsky et al., 2007; Hamilton 2010), those techniques are mostly numerically based and do not provide an insight on the physical information inherent in the wave spectrum. Therefore, in spite of the current common use of the wave spectrum, for both measured and modelled data, there is no standard procedure for its analysis. Since in the present case the spectral structure is fundamental, a new methodology has been designed with the final objective of getting a better understanding of the local wave conditions with emphasis on the temporal and spatial variability. Because of the large volume of information in each wave spectrum (order of 10^3), data reduction has to take place one way or another. To this end spectral partitioning is used. This is a technique that consists of grouping spectral bins that belong to the same physical or meteorological “event” into an entity that is then referred to as a partition and which can be more properly characterised by its own integral parameters (e.g., H_{m0} , $T_{m-1,0}$, θ_m). This procedure is explained in detail in Portilla et al. (2009).

Since a fundamental issue of this characterization is the identification of spectral wave systems in a statistical sense, from those reduced parameters a function that allows discriminating one wave system from another in an objective way is sought. This task falls thus into the clustering type of algorithms. Assuming that the wave spectrum can be properly summarised by the parameters of its partitions, these parameters (namely the peak period and peak direction) are used here to characterise the whole partition spectrum. In the present approach, the collection of these parameters for the whole spectral series is used to build their bivariate distribution as a function of frequency and direction. The result is what formally constitutes the empirical joint probability of peak frequency and peak direction of spectral partitions, which shortly accounts for the occurrence probability of spectral partitions (Eq. (2)). If the spectral series are sufficiently large, these functions become smooth and the spectral domain of each wave system can be explicitly defined. Thus at each specific location these spectral domains define the wave systems in a statistical sense.

$$\Pr(F_1 \leq f_p \leq f_2 | \theta_1 \leq \Theta_p \leq \theta_2) = \int_{\theta_1}^{\theta_2} \int_{f_1}^{f_2} g(f, \theta) df d\theta \quad (2)$$

In this equation, F_p and Θ_p represent the peak frequency and peak direction of spectral partitions respectively and g represents their empirical bivariate distribution, which is a non-negative function that satisfies the condition $\int_0^{2\pi} \int_0^\infty g(f, \theta) df d\theta = 1$. The limits of the

spectral domain ($f_1, f_2, \theta_1, \theta_2$) are determined empirically from the statistics of the spectrum.

The occurrence probability of spectral partitions gives specific information about the spectral domain of the wave systems, but it does not contain information about their energy. Therefore a parameter including energy is incorporated in the analysis, the *mean overall spectrum*, computed as the average energy of the series of each spectral bin. Further details on this methodology are given in Portilla et al. (2015, submitted for publication).

3.2. Integral parameters

While spectral variables provide very detailed information about the different wave systems, it is also useful, and still customary, to look at wave conditions in the context of the geographical space, and also from an integrated perspective. For this, typical wave parameters like significant wave height (H_{m0}) and mean wave period ($T_{m-1,0}$) of the gridded ECMWF data are computed for the whole area and for the different mooring locations as well.

4. Results from buoy data

4.1. Buoy directional spectra

The spectral buoy data are summarised through the *occurrence probability of spectral partitions* functions, which are presented in Fig. 3 for the four moorings. For the interpretation of these plots it is important to take into account the amount of data used at each location, which is given in Table 2. It can be seen that only at Tumaco and Buenaventura there are long enough data sets, containing spectra for all months, while for some locations the number of spectra is very limited. At Gorgona and Solano the spectral conditions for a few months are well represented. Another characteristic associated with the limited amount of data is the discontinuity of the functions, which makes it difficult to judge whether some spectral features are related to each other or if they correspond to different originating meteorological conditions.

The analysis will be centred at the Tumaco location, because the more consistent dataset allows identifying more features. Looking at the corresponding graph (Fig. 3a), it is possible to identify several wave systems, out of which the most important is the set of wave systems with flow directions between 60° and 80° , and frequencies greater than 0.1 Hz. Apparently, there are up to four wave systems in this sector with frequencies ranging from 0.15 Hz to 0.4 Hz, but, as just mentioned, it is difficult to judge whether these are actually different wave systems or they appear spuriously separated because of the limited amount of data. In any case, there are indications that over the Southwest Pacific Ocean different meteorological regimes lead to waves with different intensities and from different locations, which is very likely given the long fetches involved. In addition, it is also clear that the wave systems of this group are related to local wind conditions, especially those found at the higher frequencies. The second set of features, judging from the occurrence probability, corresponds to the systems with frequencies under 0.1 Hz and directions between 45° and 120° . Similarly, the continuity or discontinuity of these features is difficult to assess, but it is evident that they correspond to long swells, with a very specific frequency and direction domain. It is to be expected that waves with flow directions around 45° are originated in the Southern Pacific while those to 120° come from the North Pacific. In addition, there are important occurrences with directions of about 100° , which suggests tropical origin. Another important aspect is related to the similar frequencies of this group of wave systems. In fact, if swells propagating in different directions but with similar frequencies occur simultaneously, the buoy will have difficulties in determining the actual directions. In such cases larger directional uncertainties are expected from the observations.

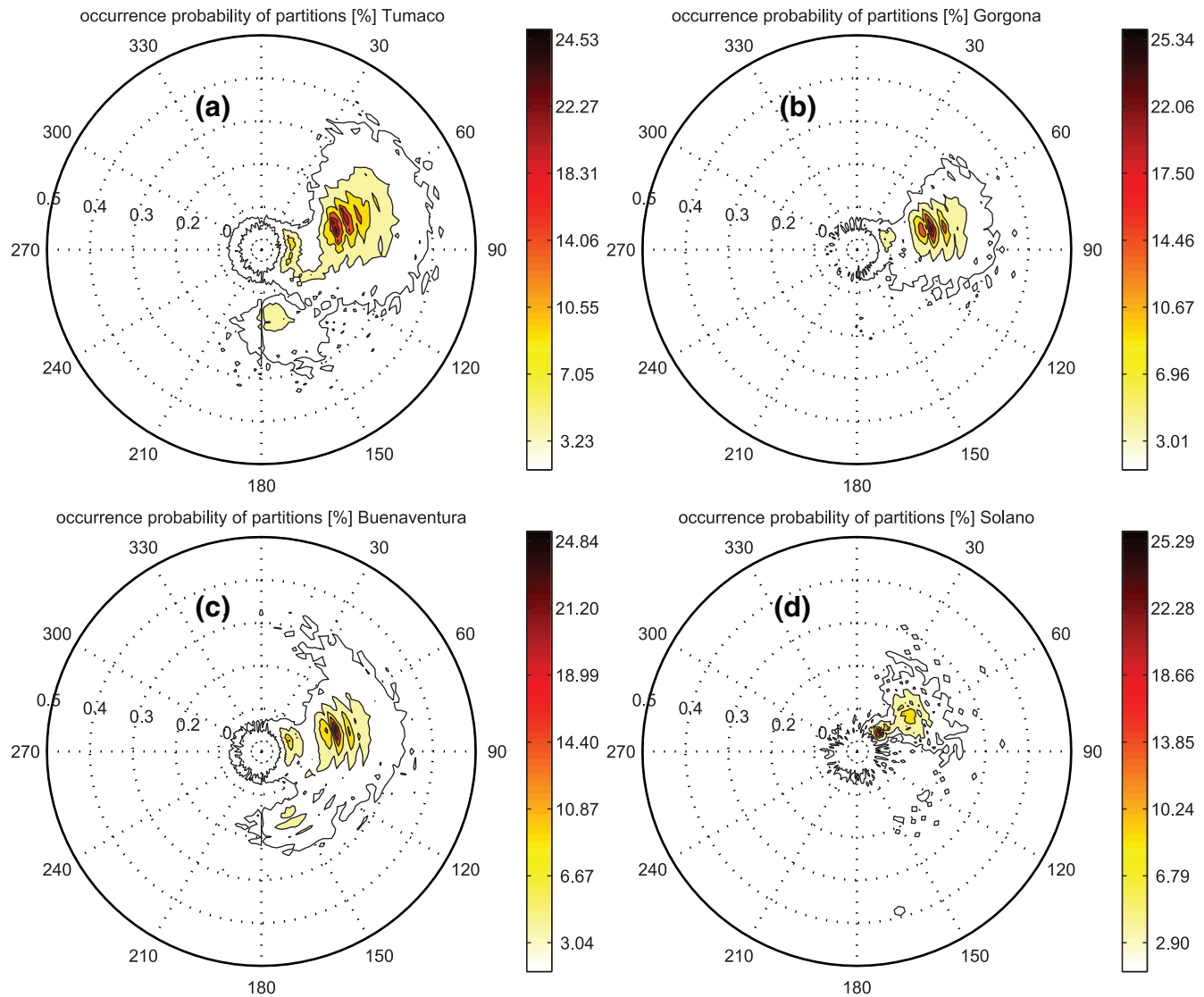


Fig. 3. Occurrence probability of spectral partitions from observed buoy spectra at Tumaco, Gorgona, Buenaventura, and Solano. In these polar plots the radial axis represents frequency in Hz and the angular axis indicates flow direction measured clockwise from North (oceanographic convention). The colour bar indicates the occurrence probability (in percentage) associated to a specific contour level. (For interpretation of the references to colour in this figure legend, the reader is referred to the web version of this article.)

Another wave feature that can be observed and seems to be independent from the two previous sets, is the one with direction to 120° and frequency from 0.07 Hz up to about 0.15 Hz. Its characteristics suggest also swell conditions, its direction indicates tropical origin. Additionally, another important wave system is the one with direction 180°, flowing southwards, and with frequency of about 0.15 Hz. This corresponds to northerly winds likely associated to the Panama wind jet. Finally, other minor features with very low frequencies and offshore directions can be observed, but these are considered spurious because they are not consistent with the geographical configuration of the region.

Similar spectral features can be observed at the other locations. At Buenaventura, the wave patterns correspond quite well with those of Tumaco. The set of wave systems flowing northeastwards are present in these data as well, but with slightly more oblique angles between 60° and 90°, and also lower frequencies (from 0.15 Hz to 0.25 Hz). Regarding the low frequency swells (lower than 0.1 Hz), only the component flowing eastwards is visible. The component flowing to South is not present. The tropical system (with 0.1 Hz and 120°) is barely visible. Finally, the wave system flowing southwards is present, but in this case with direction 150°. At Gorgona the visible features are those

flowing northeastwards (between 60° and 90°) with similar characteristics as in the previous locations. In addition, the long swell systems propagating northeastwards are clearly present. The other wave systems that were detected in the Tumaco mooring are not depicted at this location, most likely because of the limited amount of data. As the Panama wind jet occurs from November to April, practically there are no data for all those months (as can be seen in Table 2). The Solano buoy registered significant amount of data just for the month of June, so only two main wave systems are visible, the one flowing northeastwards (60°) with frequency 0.15 Hz, which corresponds to the same set of features with a similar direction found at the other moorings. The second corresponds to the long swells also flowing northeastwards (60°) and with frequency below 0.1 Hz. It should be noted that this location is sheltered from swells coming from directions larger than 120°, because of the orientation of the Central American Coast.

4.2. Buoy frequency spectra (seasonal variability)

To have an insight on the seasonal variability of the different wave systems picked up by the buoys, an analysis based on the *spectral variance density* and the *mean spectral direction* is presented, from the

Table 3

Observed wave integral parameters statistics, N is the number of records, H_{m0} is the significant wave height (in metres), $T_{m-1,0}$ is the mean wave period (in seconds).

	Start	End	N	Mean H_{m0}	Median H_{m0}	Max H_{m0}	Mean $T_{m-1,0}$	Median $T_{m-1,0}$	Max $T_{m-1,0}$
Tumaco	December 2009	December 2012	8499	1.01	1.00	2.19	6.86	6.14	17.79
Gorgona	May 2011	October 2012	3186	1.13	1.12	2.27	7.76	7.53	21.46
Buenaventura	May 2011	February 2013	7752	0.96	0.92	2.18	8.21	7.83	17.23
Solano	June 2011	July 2011	471	1.17	1.15	1.91	10.61	10.77	24.45

perspective of the frequency dependent variables directly estimated by the instrument. From the variance density it is possible to assess the energy magnitude of the different events, which is complementary to the information given by the 2D occurrence probability plots. To this end, the averages of these variables on a seasonal basis (Fig. 4) have been evaluated.

For the analysis of these figures we consider the different spectral peaks in a general sense from all the buoys. For this, the amount of data in every location should be taken into account (Table 2). Since Tumaco and Buenaventura have the longest sets, the analysis is mainly centred in these locations, although because of the geography these locations are sheltered from southerly waves. Clearly around 0.1 Hz a separation exists between different wave regimes, some occurring at lower and others at higher frequencies. The long swells already identified in the 2D plots are present in the seasonal averages of the frequency spectra.

The lower frequency peaks are more energetic in the boreal winter season (Tumaco and Buenaventura). The energy of these swells decays progressively along the months of March, April and May (MAM) and in June, July and August (JJA), and increases again during September, October and November (SON). The changes in time of direction indicate that the origin of these swells is also progressively different. Directions are between 90° and 110° during the boreal winter, indicating an important contribution from the tropics and the North Pacific. During the MAM months more eastwards directions are recorded (between 80° and 90°, indicating that the generating zone is in the tropics), and they become slightly more north-westwards (70°–80°) during the JJA months. Solano is clearly exposed mainly to southwesterly swells, with relatively large southerly waves with directions lower than 50° arriving at this location during the JJA months.

Apart from these swells, there are other peaks at very low frequencies at Gorgona, Buenaventura, and Solano. These peaks are physically possible because of the long fetches available, however the corresponding frequencies are near the cut-off frequency limit of the instrument, so it is difficult to assess whether they are real or spurious (at Tumaco these features are not present because they have been explicitly removed during data pre-processing). These spectral features require further assessment in regard to measurements.

Almost all the other peaks fall in frequency range between 0.1 Hz and 0.2 Hz. Concentrating again the analysis on the locations with higher density data (Tumaco and Buenaventura), important variations in energy and direction are observed. During December, January and February (DJF) the energy comes from directions around 120° (northwesterly) and it is relatively low. It becomes even milder during the MAM months with angles slightly lower (100°–110°). Then the magnitude increases during the months of JJA and SON, while the direction becomes more eastwards (80°–90°). Finally, looking at frequencies higher than 0.4 Hz (more directly associated to the local wind), we see that they are not directly associated with the previously analysed peaks (between 0.1 and 0.2 Hz), but in most cases they tend to flow more towards North (around 70°–80°), with a clear exemption in the months of MAM, when directions are more eastwards (around 100°). Note however that, especially in the high frequency range, noise is more easily present. Together with the likely

variability of the local winds, this leads to some non-significant variability for direction, as it is evident for Solano in panel 4 h.

4.3. Buoy integral parameters

Although wave conditions that contain two or more different wave systems, as those found in the Colombian Pacific, cannot be properly described using integral parameters from the full spectrum, still these, classically the significant wave height (H_{m0}) and the mean wave period ($T_{m-1,0}$), are commonly used. The simple reason is that they are much easier to understand and communicate. Therefore these parameters are here briefly evaluated using standard statistical descriptors (i.e., histograms, the mean, the median) presented in Fig. 5. Some of them are summarised in Table 3. In the box-whiskers plots, the box limits are set to the 25th and 75th percentiles, the red line indicates the median, the whiskers limits are set to the 1st and 99th percentiles, and the red crosses are values outside the 1st–99th percentile range, indicating potential outliers.

From Fig. 5 and Table 3 we can see that wave conditions in the study area range from low to moderate with expected values of wave heights around 1 m, and maximum values around 2 m. Wave periods range from 5 to 10 s, with maximum values around 20 s. Typical waves at Tumaco are about 1 m high with a distribution slightly skewed towards higher values. Wave periods range between 5 and 14 s with a distribution heavily skewed towards high values, which indicates the presence of high wave periods with rather lower occurrence. At Gorgona, two groups of points are apparent both in wave height and wave period (although from the previous analysis we know that there are several physical events involved). For wave height there is a lower peak around 1 m, while the overall peak is around 1.13 m. The overall peak of the period distribution is around 7 s, and a secondary peak is found around 8 s. Wave heights at Buenaventura also show a skewed distribution towards higher values, with typical values around 0.8 to 0.9 m. The mean period distribution is also skewed and has a heavy tail, with values from 5 to 14 s. At Solano the amount of available data is limited to a couple of months (June and July). Wave heights are about 1 m and wave periods around 10.7 s.

5. Results from the ECMWF model data

5.1. Overview of spectral wave systems

The occurrence probability of spectral partitions is also used to characterise model data. The advantage in this case is the large dataset, from whose derived functions become smooth and wave systems can be clearly defined and depicted. An overview of the possible wave systems is given considering a single location, namely the grid point with coordinates 4°N, 78°W. This location was selected because of its central position and its proximity to Buenaventura for a possible association with the observed data. From this overview, the spatial and temporal variability analyses will become simpler. The resulting wave systems are presented in Fig. 6 and summarized in Table 4.

According to their occurrence probability many possible wave systems can be identified. It should be noted that in fact, more

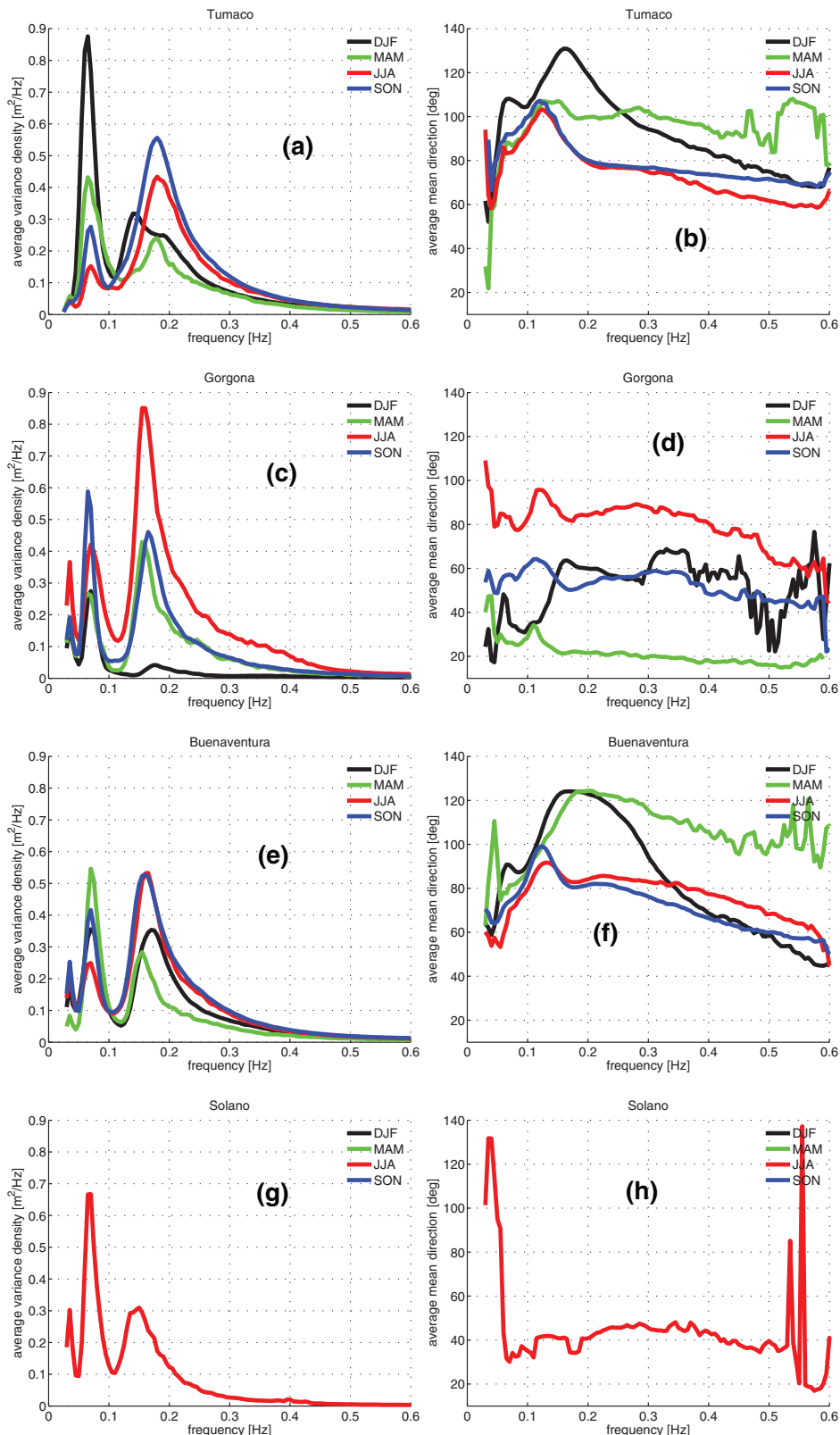


Fig. 4. Seasonal averages of the frequency dependent variables, variance density (left) and mean direction (right) at the mooring locations Tumaco (a, b), Gorgona (c, d), Buenaventura (e, f), and Solano (g, h). See Table 2 for the data density used. (For interpretation of the references to colour in this figure legend, the reader is referred to the web version of this article.)

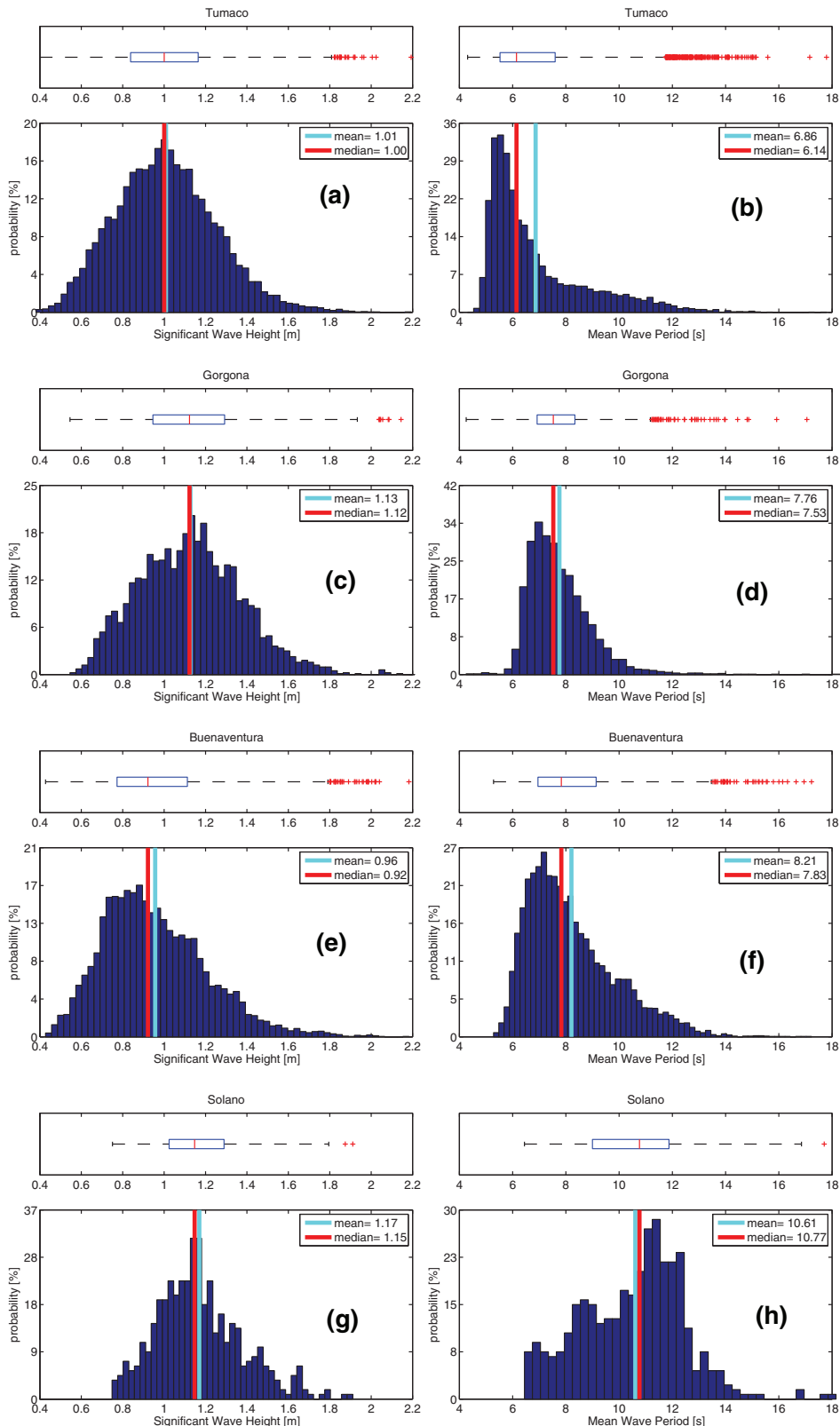


Fig. 5. Histograms and box-whiskers plots of total significant wave height (H_{m0}) and mean wave period ($T_{m-1,0}$) at the mooring locations Tumaco, Gorgona, Buenaventura, and Solano. (For interpretation of the references to colour in the text, the reader is referred to the web version of this article.)

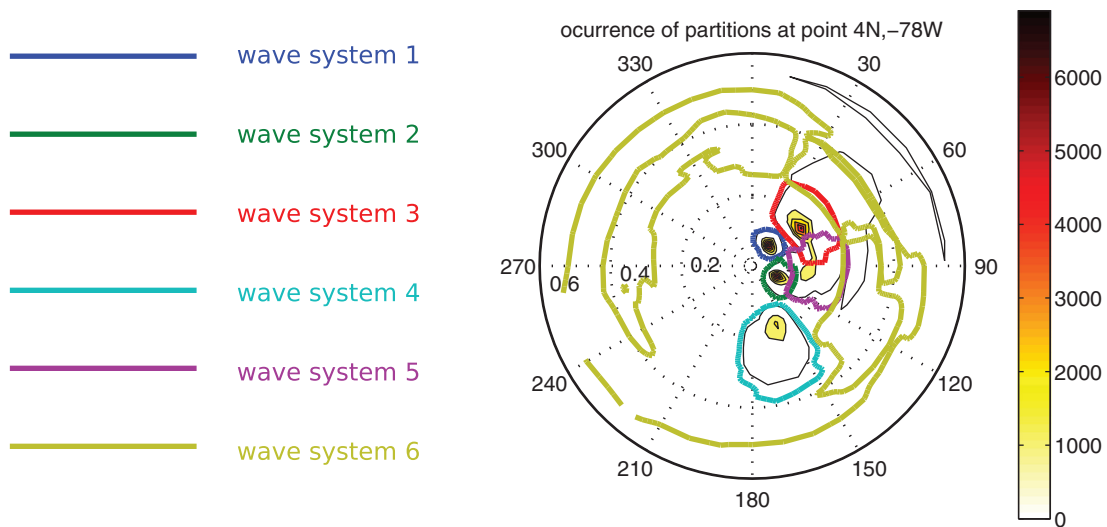


Fig. 6. Wave systems found at the Colombian Pacific for the modelled reference point 4°N, 78°W. The polar plot uses oceanographic convention, with flow direction measured clockwise with respect to North. The radial axis corresponds to frequency, ranging from 0 to 0.6 Hz. (For interpretation of the references to colour in this figure legend, the reader is referred to the web version of this article.)

Table 4
Summary of the representative wave systems in the Colombian Pacific, shown in Fig. 6.

Wave system	Peak frequency	Peak direction	Deep water wave length	Colour
1	0.074 Hz	37.5°	285 m	blue
2	0.074 Hz	112.5°	285 m	green
3	0.1745 Hz	52.5°	51 m	red
4	0.1745 Hz	157.5°	51 m	cyan
5	0.1586 Hz	97.5°	62 m	purple
6	>0.3 Hz	Several	17 m	yellow

than twenty distinct wave features are detectable from the occurrence probability matrix. However, some of them are very close to each other and can be treated as a single one, and many others are located at frequencies above 0.3 Hz and are considered as a single wind-sea system. Among the most important features, five main wave systems plus the high frequency wind-sea components can be distinguished. These are indicated with different colours in Fig. 6. The first wave system is the one with low frequency (0.07 Hz) flowing northeastwards, which has swell characteristics and has been contoured in blue. The second swell at low frequencies and flowing southeastwards is contoured in green. Number 3 flows northeastwards and is found at higher frequencies (0.17 Hz, red). The fourth system has similar frequencies as number 3, and it includes higher frequency components as well, and flows southwards, contoured in cyan. The fifth wave system has relatively low frequencies (0.15 Hz) and flows eastwards. This gives an indication of tropical origin, and it is contoured in purple. Besides these five systems, other features with lower occurrence probabilities can be detected from the data, at relatively higher frequencies and flowing almost in all directions, but preferentially northeastwards, westwards, including systems flowing offshore. Because of their characteristics, we associate all these systems to wind-sea conditions.

In the present approach the wave characterisation is made on the basis of the signature of the spectral statistics. However, this characterisation is not purely numerical because the wave spectrum contains a lot of physical information about the local conditions. This characteristic is what we want to exploit here through the spectral statistics. From the long term series the data tend to cluster and spontaneously define different domains supporting the idea of the existence of these wave systems and the fact that can be differentiated. More in general, a classification can be done on the basis of the magnitude of the wind forcing (e.g., wind-sea or swell). A typical approach is to compare the wind and wave speed using the wave-age

criterion (Eq. (3)).

$$\beta = \frac{c_p}{U_z \cos(\theta - \psi)} \quad (3)$$

where c_p is the wave phase speed (for deep water), U_z is the wind velocity at height z , 10 m in this case, and θ and ψ are the wave and wind directions respectively. Commonly, a value of β below 1.3 has been used to indicate that waves are part of a system being forced by wind (e.g., Donelan et al., 1985; Hasselmann et al., 1996; Drennan et al., 2003).

In order to assess the degree of wind forcing on the presented wave systems, the wave age parameter (β) has been calculated from the whole time series of wind and wave spectra. The results are shown in Fig. 7. There we can see that the wave systems WS1 and WS2 are clearly above the 1.3 threshold. According to this criterion they can be labelled as swells. This condition is less clear for wave systems WS3 and WS5. In most cases these systems are above the 1.3 limit, but there are also cases below. As a whole these wave systems can be regarded as old wind seas (or young swells). The wind forcing is more evident for the wave system WS4, under the influence of the Panama jet. However, for this system there is a considerable number of waves with a high wave age number, i.e., the tail of its distribution is rather heavy. This can be associated to the jet characteristics; in general, winds in the channel are funnelled with their intensity decreasing further away from the coast. The jet also turns anticyclonically to the west to adjust to the geostrophic forcing (Chelton et al., 2000a, 2000b). From these effects, waves get relaxed from wind forcing showing thus larger wave age numbers. As for the WS6 group, it is clearly seen that they are being forced.

The subtle distinction, if any, between "old wind sea" and "young swell" deserves a specific comment. Clearly the transition can only be gradual, no step distinction is possible, and indeed, as it should be, there is no accepted boundary wave-age value from one to the other.

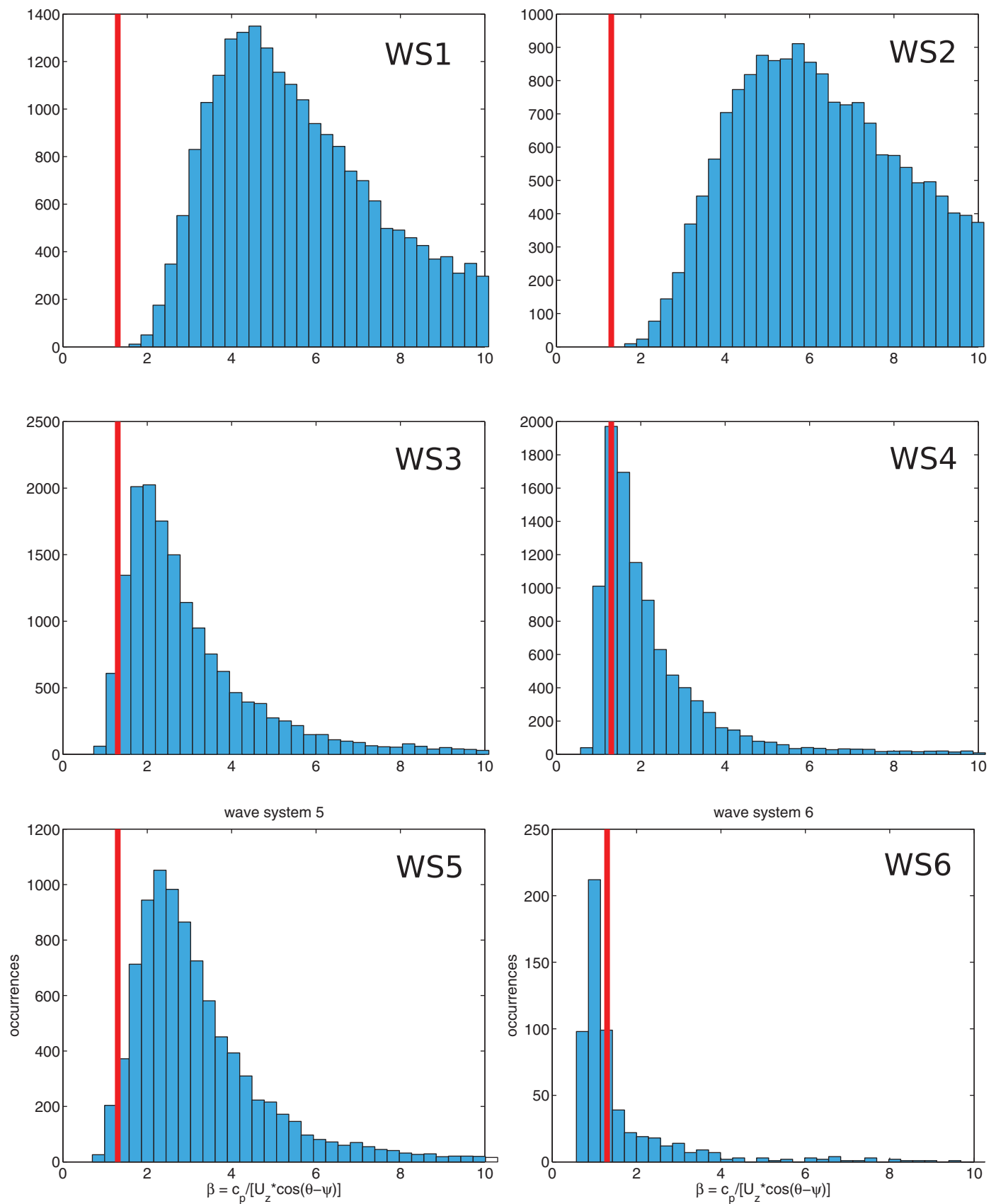


Fig. 7. Wave age parameter for the six wave systems found in the Colombian Pacific. The red line indicates $\beta = 1.3$, for values below the line waves are considered to be forced by wind. (For interpretation of the references to colour in this figure legend, the reader is referred to the web version of this article.)

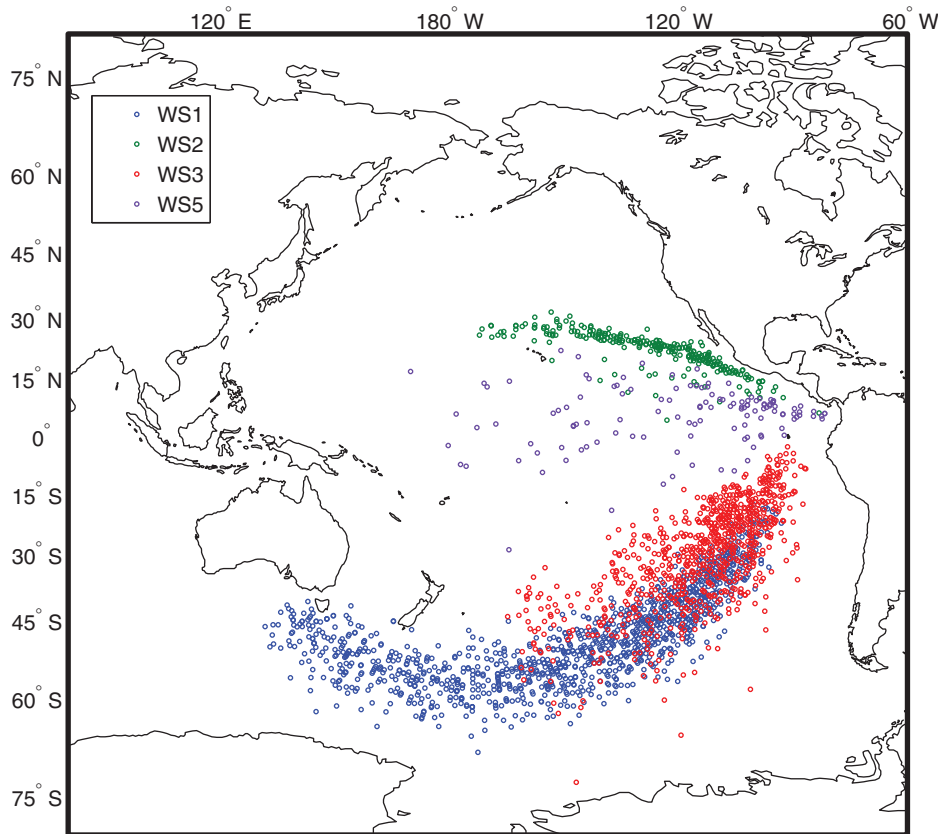


Fig. 8. Location of the source points of swells arriving into the Colombian Pacific area. The colours refer to the wave systems defined in Fig. 6 and Table 4. (For interpretation of the references to colour in the text, the reader is referred to the web version of this article.)

The truth is that in the large majority of cases we are not dealing with a monochromatic system. Therefore for practical purposes it is a matter of seeing where, i.e. on which frequencies, most of the energy is located. It is also in this respect that the method we describe in this paper shows and proves its usefulness. The long term statistics of the partitions is capable to highlight and distinguish between systems that would be indistinguishable in the plain spectral representation. Trivial as the distinction could be in the single spectrum, it may become important when we consider the long term effects of waves on, e.g., the various coastal systems and, the more so, when we need to understand the genesis of each wave system.

The occurrence probability function of the model (Fig. 6) shows spectral features that are qualitatively consistent with those from the buoys, especially with those with higher data densities (Tumaco and Buenaventura, Fig. 3a and c). For instance, waves corresponding to the Panama wind jet are also present in both locations. The southwesterly wave systems (WS1 and WS3) are visible in all locations, while the northwesterly (WS2) swell systems and the tropical wave system (WS5) are apparent only at Tumaco. The main limitation in the case of buoy data is the relatively short time coverage. Nevertheless, the consistency of the overall picture is encouraging because this way of looking at the local wave climate gives a better insight of the physical processes represented by the model allowing for a more detailed spectral comparison, regardless of the purpose.

In addition, the origin of these different wave systems can be estimated backtracing the swell sources (e.g., Portilla, 2012). According to the dispersion relationship, waves disperse in frequency, and they spread in direction while moving away from the source point. As a consequence, the swell peak frequency recorded at a given remote location shifts in time to higher frequencies (e.g., long waves arrive first followed by shorter waves). This peak frequency–time dependency can be associated to the distance from the origin. In addition,

information about the travel direction is contained in the spectrum itself. The result of this evaluation is given in Fig. 8 for the wave systems WS1, WS2, WS3, and WS5 that exhibit more regularly swell characteristics. For the present estimation, only wave systems that reach at least 0.5 m significant wave height, and obviously a positive slope in their relationship peak frequency versus time, are considered. Events containing a too low number of time sequences were discarded because the algorithm is very sensitive to the number of points considered in this relationship.

As it can be seen in Fig. 8, the sources of swell encompass a large area, with most events originated in the southern hemisphere. From this perspective, it is not clear that wave systems WS1 and WS3 are independent. Their generation zones overlap over a large area around latitude 40°S. The fact that they appear distinct in the spectral domain is thus related to the combined characteristics of wind intensity and fetch that characterise their generation. In any case, the spectral characteristics show clearly that significant differences exist between the two regimes. The spatial domains of the other wave systems are more clearly defined. System WS2 originates in the northern hemisphere, between 10° and 30° north, while system WS5 is more related to tropical conditions. Therefore, the sequential relevance among wave systems WS2, WS3, WS4, and WS5 is expected to be driven by the dynamics of the trade winds and it is thus markedly seasonal.

It should be noted however that trade winds in the ITCZ are expected to blow southwestwards (SW) in the northern hemisphere and northwestwards (NW) in the southern hemisphere. The present results are thus in apparent contradiction with this trend. A possible explanation is that winds in the Colombian Pacific are affected by geographic and orographic features. Actually the Panama wind jet can be associated to the SW stream and this particular direction (SW) is more evident close to the Papagayo and Tehuantepec jets. Similarly, the NW flow can be detected in further offshore and southern

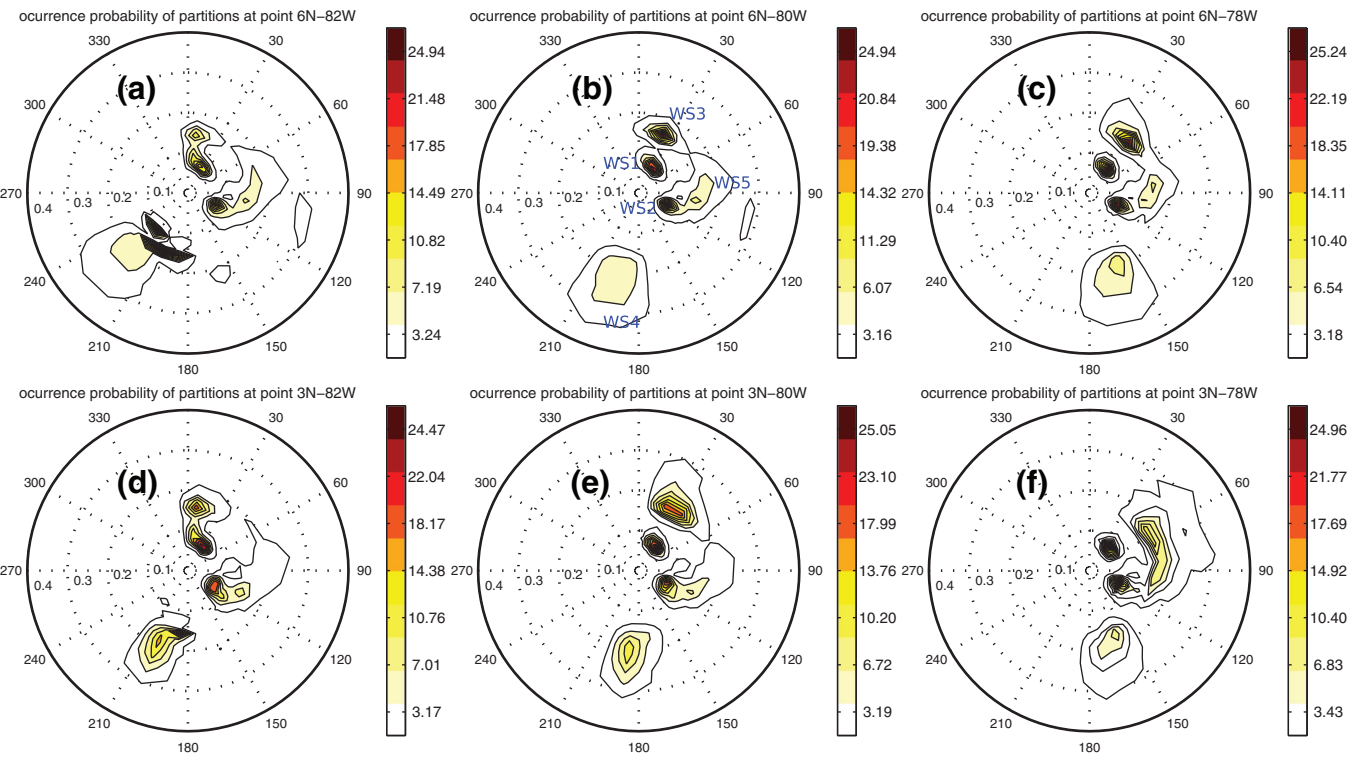


Fig. 9. Occurrence probability of spectral partitions for the ECMWF grid points. The radial axes are the frequencies and angular axes indicate directions in degrees, oceanographic convention. The colour scale indicates the number of occurrences as percentage of the total. The wave systems have been labelled in one of the panels to facilitate reading. (For interpretation of the references to colour in this figure legend, the reader is referred to the web version of this article.)

locations outside the present study area (not shown). A global mapping of the occurrence probability spectra should elucidate more clearly this spatial variability.

5.2. Spatial variability of the ECMWF spectra

Having an overview of the main wave regimes described above, the spatial regional wave climate can be assessed. Two indicators are used to this end, namely, the *occurrence probability of spectral partitions* (Fig. 9), and the *mean wave spectrum* (Fig. 10), computed over the study period (1979–2013).

From the occurrence probability of spectral partitions (Fig. 9), the six wave systems referred to can be identified (for conciseness, only the grid points showing the larger differences are considered). The two wave systems with lower frequencies flowing northeastwards and southeastwards (WS1 and WS2) are spatially consistent at all the points (in frequency and direction), only at the most offshore locations they slightly lose relative importance compared to the systems flowing southwards. Contrarily, the third system (WS3) varies significantly in space. At the near-shore locations, from north to south the angle increases from 30° to 60°, while it loses relative importance. These variations can neither be attributed to the geographical configuration nor to bathymetric effects, because, should this be the case, the longer swell system (WS1) would then be affected to a larger extent (because the longer waves are expected to interact more with bathymetry). Therefore, it is more likely that those variations are associated to the wind field conditions. The site is closer to the generation source so that directional dispersion is present at the spatial scale of the region. This is supported by the fact that this behaviour (i.e., WS3 becoming more oblique from north to south) can be observed along the columns from near-shore to offshore, and certainly the offshore locations are not affected by bathymetry. Similarly, the wave system flowing southwards (WS4) is also subject to large

spatial variations. From near-shore to offshore (all columns) its direction changes from about 165° ($\pm 15^\circ$) to 225° ($\pm 15^\circ$). Moreover, at the offshore locations not only this system becomes more important and even dominant, but also its configuration becomes more complex, with up to four sub-systems clearly defined in some points. These large spectral-spatial differences and the existence of other systems flowing in the same direction indicate that the region is constantly under the influence of wind. It is also likely that the offshore locations are exposed to more than one wind regime. From this wave system, the low frequency of one of the sub-components (near 0.1 Hz) is remarkable (see Fig. 9a). Given the relatively shorter fetch of this system in comparison with the wave systems originating in the open ocean (WS1 and WS2), it is likely that the low frequencies are due to strong local wind conditions. This low frequency system vanishes towards the southern points because of the fanning out of the wind jets. The other relevant wave system (WS5), flowing eastwards, is also consistent at most locations. The difference is that at the southern locations it tends to be composed of two sub-systems, a principal one, propagating slightly more southeastwards, and another with propagation direction truly to 90°, albeit with low occurrences (under 3%). Finally, as already seen from Fig. 7, higher frequency wave systems (locally generated) can be seen in different directions, but with low occurrence values (under 3%). An apparent trend is that at the northern and offshore points there are systems flowing to southeast (see Fig. 9a, features flowing to 100° and 160°), while at the southern near-shore points the systems flowing to northeast are more clearly visible (see panel f, lobe of WS3 flowing to 60°).

As seen from Fig. 9, the occurrence probability of spectral partitions proves very skilful to highlight details of the spectral wave climate. Using this indicator, the spectral features appear clearly defined. Not necessarily all the spectral features that appear there may be relevant for all applications because what is given by this parameter is the relevance of wave patterns according to the number of

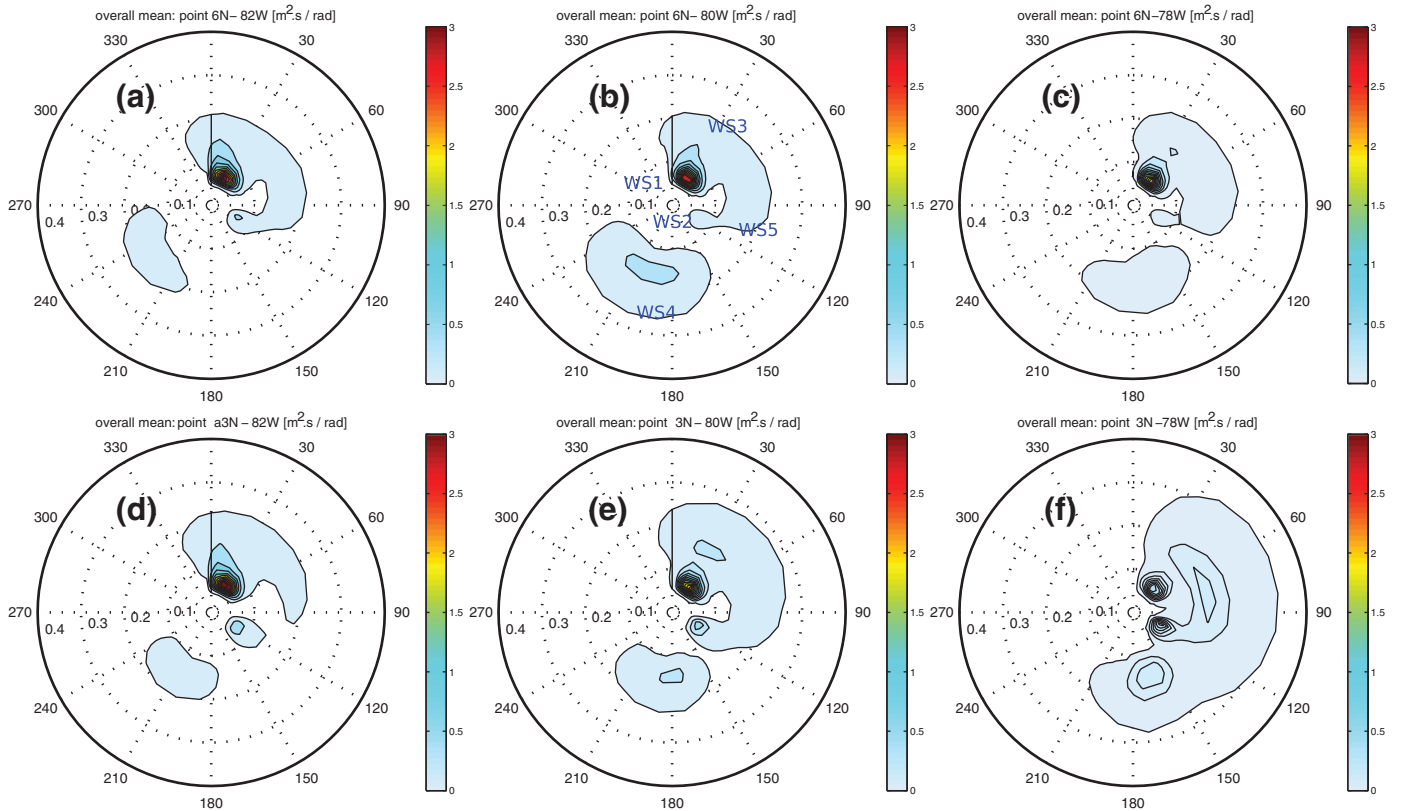


Fig. 10. Average 2D spectrum for the ECMWF grid points. The colour scale indicates the variance density levels. (For interpretation of the references to colour in this figure legend, the reader is referred to the web version of this article.)

occurrences. Therefore for a more complete description, information on energy levels is needed. In the present case this information is given in spectral form by the average wave spectrum. This can be seen in Fig. 10 for the same ECMWF grid points shown in Fig. 9. It should be noted that the frequency domains of wave systems in Figs. 9 and 10 are slightly different because of the different spectral signatures of the two indicators.

It can be seen from Fig. 10 that the picture given by the average spectrum is rather different from that of the occurrence probability, not only because the variable is different, but also because parameters like the average (of energy in this case) tend to smooth details. In Fig. 10 clearly the most energetic system, in average sense, is the one flowing to northeast (WS1), with the highest values in the most offshore (left) and north (top) locations. At the near-shore points the energy of this system is significantly lower, likely due to the obstruction from the southern peninsulas. The second most energetic system depends on the specific location. For instance, the swell system flowing southeastwards (WS2) is visible in all southern points, while in the central points the wave system flowing southwards (WS4) is also energetic. In turn, towards the near-shore points the system flowing northeastwards (WS3) is also important. About this system, it can be seen that in the offshore locations it is not clearly separated from the first system (WS1), while this separation is clearer in the near-shore points. On the other hand, the tropical wave system (WS5) does not appear well defined using this indicator in contrast with its occurrence. This means that WS5 is a system that is present regularly, but with low energy in the mean. It appears more as background energy of the first and second wave systems and is more noticeable in the near-shore southern points. Finally, the high frequency energy components are relatively more relevant in the near-shore locations, with components flowing mainly northwestwards and westwards (not shown in Fig. 10).

5.3. Time variability of the ECMWF spectra

The time variability of these spectral features is assessed using the mean 2D spectra, and also from the point of view of integral parameters. For this the analysis is centred at the grid point 4°N, 78°W.

Fig. 11 shows that there is a marked temporal dependence of the wave climate. During the boreal winter months (December, January, February) the swell system flowing southeastwards (WS2) is the most energetic, but it decays significantly from March on. The wave systems flowing northeastwards and eastwards (WS1, WS5) are active the whole year, but WS5 is specially energetic during the second half of the year (from July to December). WS3 is insignificant from January to April. Also the wave system flowing southwards (WS4) is constantly present from November until May. Finally, the low energy offshore wind-sea system (WS6) is visible in May, and February. The summary view of this seasonal variability in terms of integral parameters (H_{m0} , and $T_{m-1,0}$) is given in Fig. 12.

This figure gives an overview of the combination of wave systems along the year. In terms of wave height, the wave system WS1 peaks in June, although from the H_{m0} point of view the system WS3 is the most energetic. This system peaks in October–November, together with WS5. The reason why these systems seem very energetic in these plots, and less significant in the 2D spectra plots, is that they are more associated to the local wind conditions. Therefore they have larger spectral energy dispersion than the other systems, hence a large integrated total energy. Consistently, their periods are significantly lower than those of WS1 and WS2. The WS2 system peaks in January and has the lowest values in July. WS4 peaks in February and reduces significantly from June to October. Finally the wave system WS6 does not present a regular pattern as the previous ones, mainly because all the wind-sea regimes are associated to this unique wave system. In spite of the low average values of these wind components,

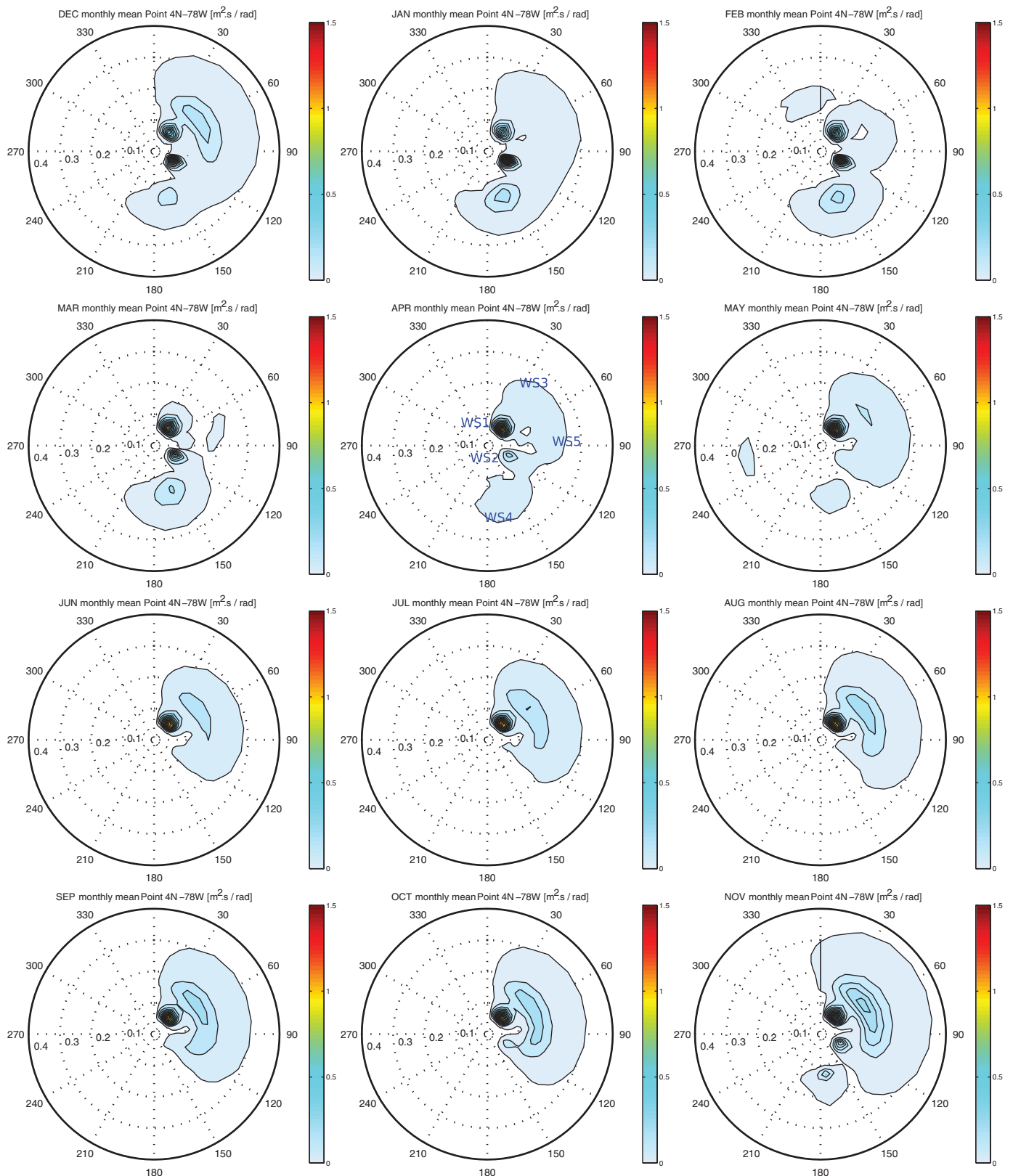


Fig. 11. Monthly variability of the 2D spectrum for the reference point 4°N, 78°W. (For interpretation of the references to colour in this figure legend, the reader is referred to the web version of this article.)

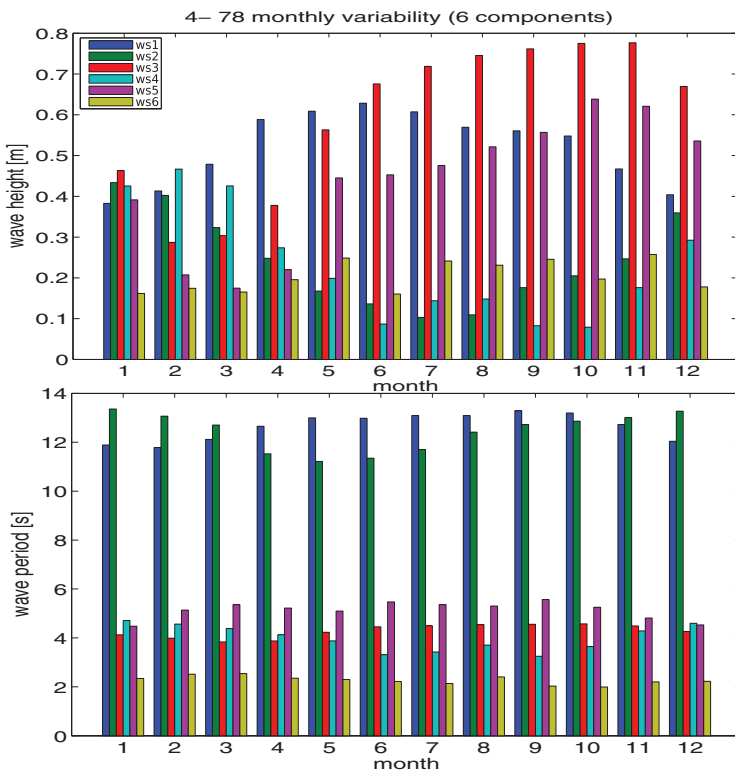


Fig. 12. Monthly variation of the integral parameters H_{m0} (top) and $T_{m-1,0}$ (bottom) for the main wave systems found in the Colombian Pacific for the reference point 4°N, 78°W. Each system is represented with a specific colour as defined in Fig. 6. (For interpretation of the references to colour in this figure legend, the reader is referred to the web version of this article.)

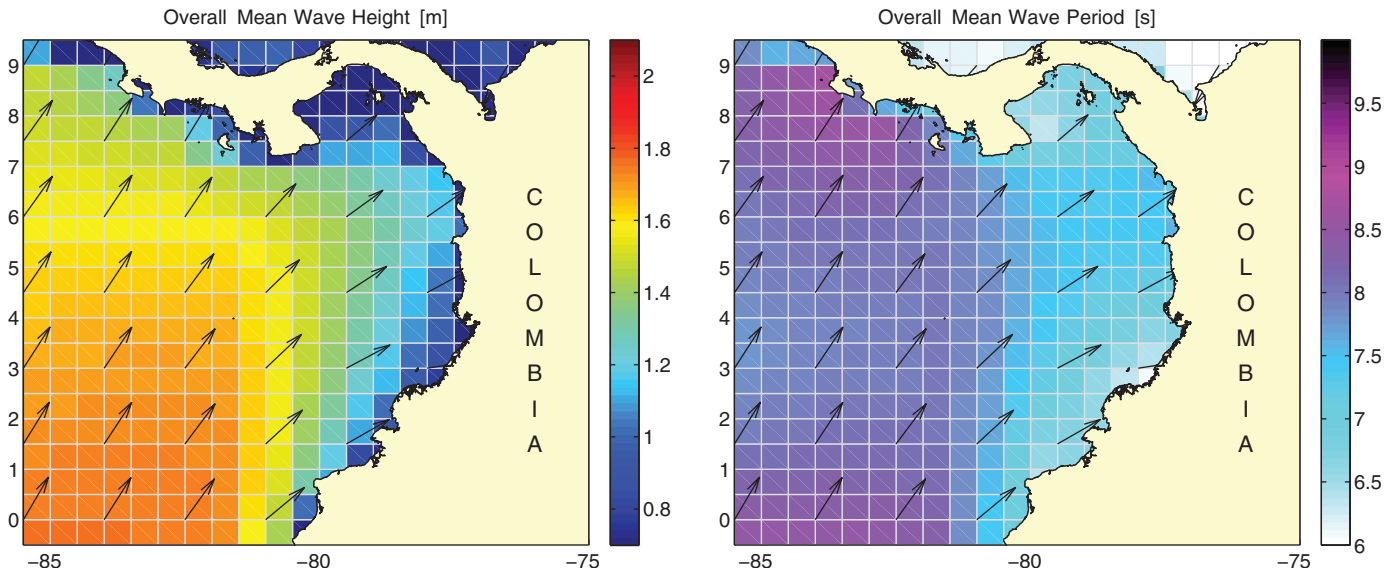


Fig. 13. Spatial mean wave height (H_{m0}) in metres, and wave period ($T_{m-1,0}$) in seconds for the period 1979–2013. The vectors indicate the mean (vectorial) direction. (For interpretation of the references to colour in this figure legend, the reader is referred to the web version of this article.)

single and specific events can be very energetic. In terms of wave periods the first two wave systems show clearly swell characteristics (large periods, and consequently large wave lengths), while the rest have lower periods, so to a larger extent they are expected to be associated to the local wind.

5.4. Spatial distribution of ECMWF integral parameters

As mentioned before, integral parameters remain commonly used because they can easily be presented in the form of maps to show

the overall spatial gradients. In addition, knowing beforehand the characteristics and the variability of the spectra at different sites, this information is very useful and complementary.

Fig. 13 shows the overall average wave conditions in the Colombian Pacific. In order to give an idea of the spatial seasonal variability from the integral parameters point of view, also monthly averages of H_{m0} and $T_{m-1,0}$ are presented in Figs. 14 and 15 respectively. In Fig. 13 it can be seen that on average wave conditions in the whole region are of moderate magnitude of about 2 m offshore. Wave period varies around 8.5 s in the offshore zone. The black arrows indicate mean

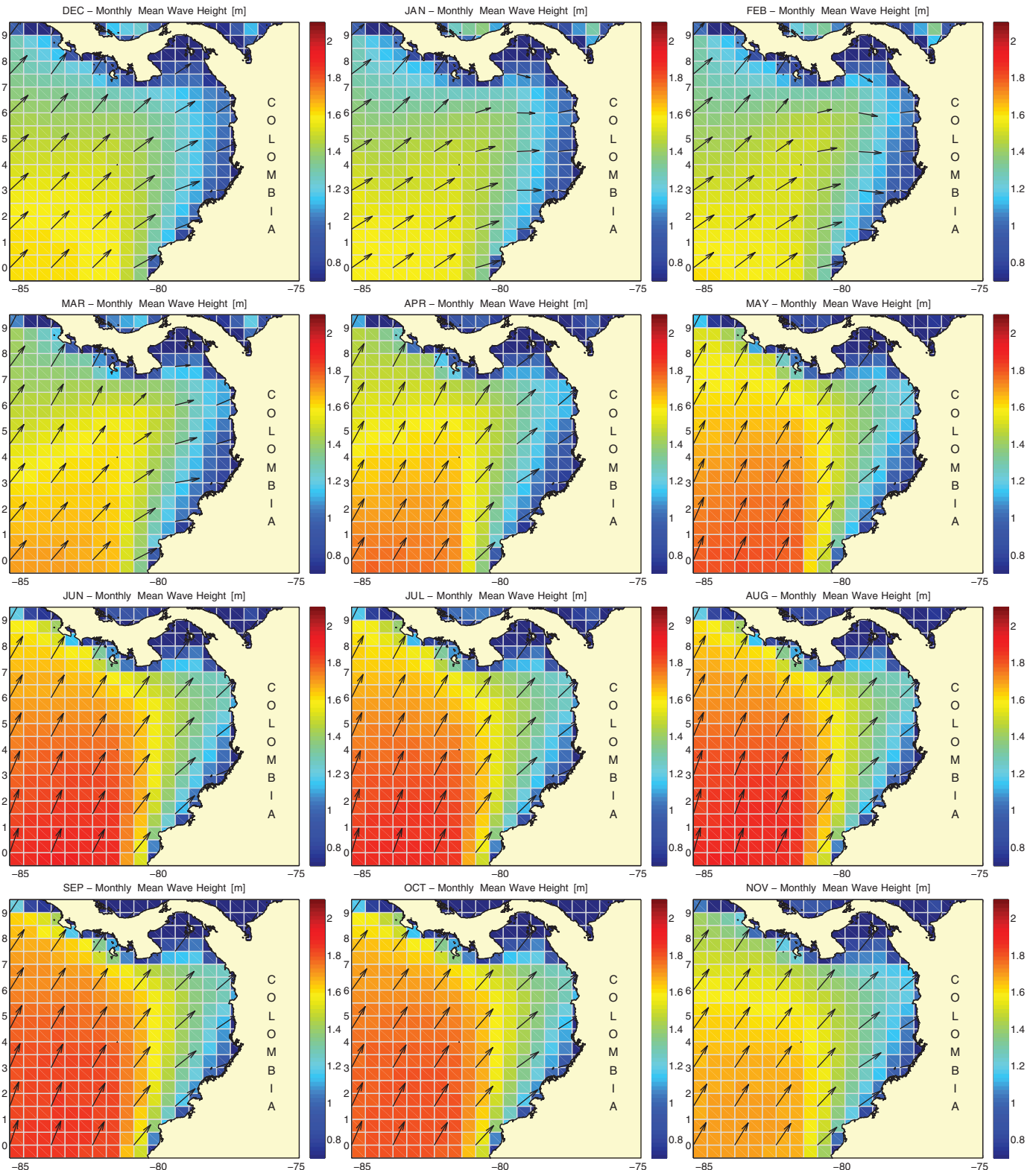


Fig. 14. Spatial monthly mean wave height (H_{m0}) in metres for the period 1979–2013. The vectors indicate the mean (vectorial) direction. (For interpretation of the references to colour in this figure legend, the reader is referred to the web version of this article.)

wave direction. Northeastwards waves dominate the average conditions, although it is expected that the exposure of the coastal zone to waves should be mainly associated to the orientation of the coastline. For instance Solano bay is exposed mainly to southwesterly waves, while most other locations are exposed to northwesterly ones.

From Figs. 14 and 15 it can be seen that waves in the region have higher H_{m0} values during the months of the austral winter (June, July, August), but the months of March, April, and May also show important swell activity, associated to the larger magnitudes of wave period. In turn, during the months of the boreal winter

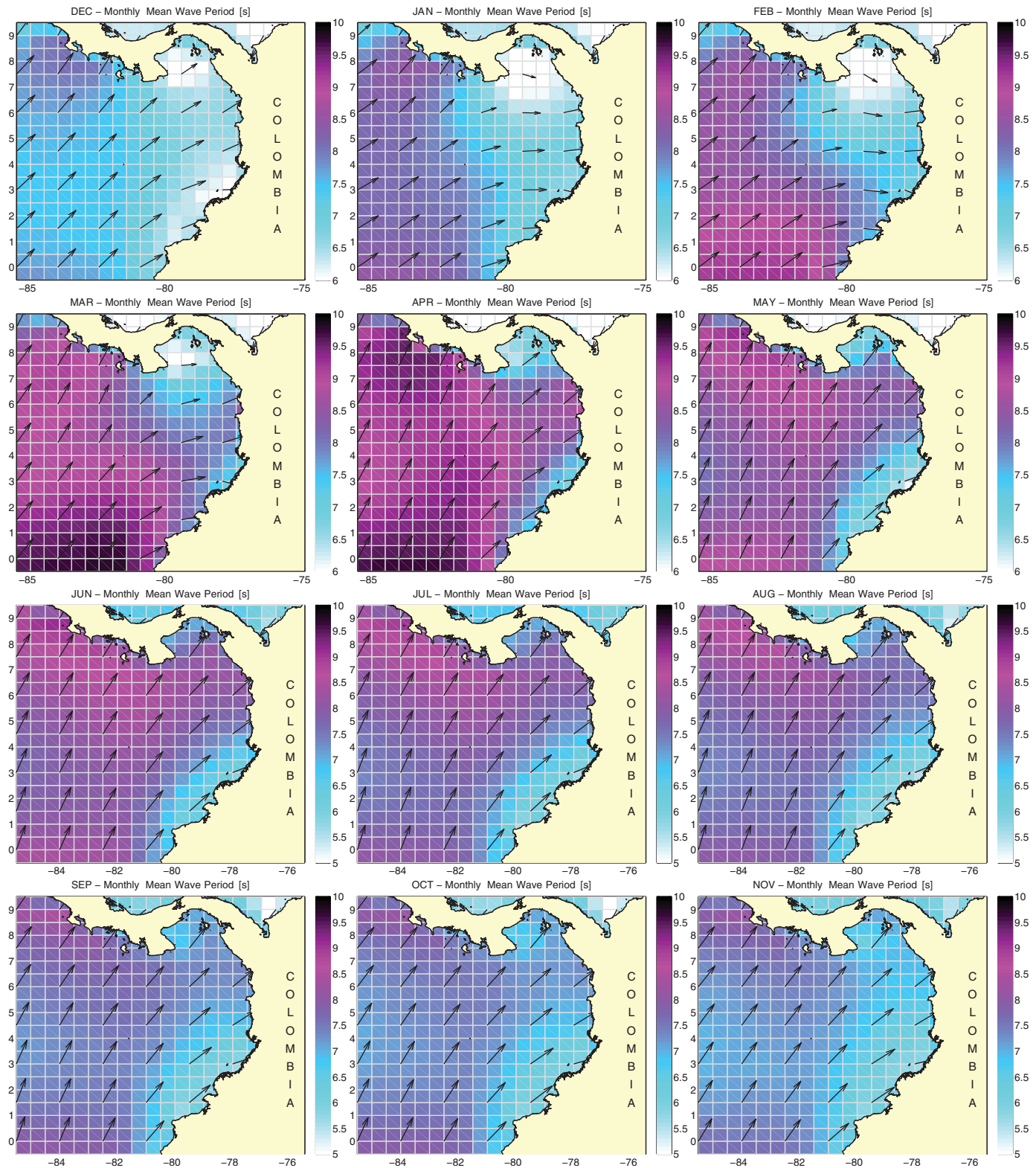


Fig. 15. Spatial monthly mean wave period ($T_{m1,0}$) for the period in seconds 1979–2013. The vectors indicate the mean (vectorial) direction. (For interpretation of the references to colour in this figure legend, the reader is referred to the web version of this article.)

(December, January, February) waves seem to be characterised by significant wind activity, specially in the north part of the domain (i.e., Panama region) and also along the coast in the southern part (e.g., Buenaventura). This is assessed from the lower magnitude of the wave periods. However, we stress again that the general patterns near-shore could be significantly different from the conditions off-

shore because of the geographical configuration. Concerning wave direction, we see that northeastwards waves are always dominant. The boreal winter months are characterised by eastwards waves, especially in the cells closer to the continent. In fact, we should note that these arrows represent the resulting vector of components with directions northeastwards, southeastwards, and truly eastwards, so

the resulting direction may reflect the relatively higher importance of southeastwards waves. As mentioned before, looking only to overall integral parameters can be misleading, because they cannot show if there is more than one wave system.

6. Summary and conclusions

At present, the characterisation of waves based on integral parameters (typically H_{m0} , $T_{m-1,0}$, θ_m) imposes severe limitations on wave data analysis. Although integral parameters do provide a good overall idea of the wave conditions for unimodal seas, they hide a lot of valuable information contained in the wave spectrum. Therefore, when two or more wave systems characterise the local wave climate, integral parameters become imprecise and even ambiguous. This is a serious drawback considering that at present the wave spectrum is the standard variable for wave description, both in models and observations. In the present work, partitioning techniques are exploited to derive statistics of the spectral series and to derive spectral indicators to describe wave conditions.

For identification of spectral wave features, the 2D spectral indicator associated to the occurrence probability of spectral partitions has shown very good skill. The clusters found from this empirical function contain information that can be related to physical characteristics (e.g., spectral characteristics, meteorological genesis, wind forcing, among others). In addition, this function provides an objective base to define the spectral domain of each wave system. Apart from its skill to define the spectral domains, this indicator does not directly display information about energy. Therefore this is complemented using energy based parameters from the 1D and 2D spectra.

Wave conditions in the Colombian Pacific are rather complex because of the many different wave systems present. Six main wave systems were identified, two of them with swell characteristics (narrow spectral bands, frequencies lower than 0.1 Hz, and wave age parameter β above 1.3, see Fig. 7), but different origins. The first one (WS1) flows northeastwards, while the second (WS2) flows southeastwards. These waves are originated outside the study area, in the South and North Pacific respectively. There is a third wave system (WS3) flowing northeastwards with directions similar to the first swell system, but with higher frequencies (about 0.2 Hz). Its characteristics suggest that it is influenced to some extent by the regional winds. There is another set of waves flowing southwards (WS4) and originated by the Panama wind jet. This is influenced by the wind to a larger extent. A fifth wave system (WS5) is found to flow eastwards. As expected, it shows high magnitudes in specific months (October–November). Finally, a whole range of wind sea conditions (WS6) is depicted covering a whole range of directions. This indicates complex gradients of the wind fields in the study area.

The spectral patterns found in the two main data sources (i.e., buoy and model data) are qualitatively consistent. Although from the buoy data it is possible to detect more sub-systems than from the model data, it is not possible to assess whether these are actually separated or if they are spurious features due to the relatively limited amount of observed data. Nevertheless, the overall consistency gives confidence about the wave systems described, and also about the robustness of the methodology.

Concerning the temporal variability, wave conditions are rather constant throughout the year, but the source of the waves changes considerably. During the boreal winter months the northerly wave systems are very active and energetic. They decay significantly during the austral winter months when the southerly systems become dominant. During the months of March–April, a combination of conditions might occur with different wave systems of significant magnitude occurring together. The October–November months show also highly energetic waves flowing northeastwards and eastwards and associated to the local wind conditions. Although on average the wave

conditions in the study area vary between moderate and low, possible combinations of wave trains may result in high wave conditions.

Acknowledgements

The development of this study has been possible with the support of many people and institutions. We are particularly grateful to Dirección General Marítima de Colombia, and Centro de Investigaciones Oceanográficas e Hidrográficas del Pacífico (DIMAR-CCCP), especially to its director Captain José Manuel Plazas Moreno for all the institutional and technical support. This study has been funded in the framework of the project *Implementación operacional del sistema de modelamiento hidrodinámico y de oleaje para la Cuenca Pacífica Colombiana*. The observed buoy data have been collected and delivered in the framework of the project *Sistema de Medición de Parámetros Oceanográficos y de Meteorología Marina* (SMPOM) also executed by DIMAR-CCCP. The model data derive from the archive of the European Centre for Medium-Range Weather Forecasts, for which we very much acknowledge the valuable support of Luciana Bertotti. We also express our gratitude to the colleagues from the operational oceanography department at DIMAR-CCCP, especially to Javier Enrique Gomez Torres, Jesús Peñaranda, and Ricardo Romero for their help with data processing and analysis. The contributions of Jeison Sosa and Sadid Latandret in related works are also very much appreciated. Special thanks are also expressed to Universidad San Francisco de Quito (USFQ), and particularly to Diego Quiroga and César Zambrano. We are also obliged to Universidad Tecnológica de Bolívar (Cartagena) for the institutional and administrative support, and to Ricardo Torres Parra (DIMAR) and Rodny Martínez (Centro Internacional para la Investigación del Fenómeno del Niño) to help promote the present study. We are also very much thankful to the anonymous reviewers whose dedicated comments contributed to improve the final manuscript. Luigi Cavaleri took part to this study as part of the EU funded My-Wave project, Theme (SPA.2011.5-03).

Appendix. Integral parameters of the wave spectrum

Integral parameters are based on the moments of the wave spectrum defined as:

$$M_n = \int_0^{2\pi} \int_{f_1}^{f_2} f^n F(f, \theta) df d\theta \quad (A1)$$

where M_n is the n moment, f_1 and f_2 are the cut-in and cut-off frequencies respectively, F is the variance density (i.e., the wave spectrum), f is frequency, and θ is direction.

The total variance of the spectrum corresponds to the moment zero and is given by:

$$E_m = \int_0^{2\pi} \int_{f_1}^{f_2} F(f, \theta) df d\theta + e_{hf-tail} \quad (A2)$$

where $e_{hf-tail}$ is the energy in the high frequency tail of the spectrum above the cut-off frequency (f_2) according to WAM code. Assuming a -5 power decay rate with frequency the energy in the tail can be obtained as:

$$e_{hf-tail} = \frac{f_2 d\theta}{4} \int_0^{2\pi} F(f_2, \theta) d\theta \quad (A3)$$

The significant wave height based on the total variance is given by:

$$H_{m0} = 4\sqrt{E_m} \quad (A4)$$

The mean wave period based on the zero and first moments of the spectrum is:

$$T_{m-1,0} = (f_{m-1,0})^{-1} = \frac{\int_0^{2\pi} \int_{f_1}^{f_2} F(f, \theta) f^{-1} df d\theta}{E_m} \quad (A5)$$

The mean vectorial wave direction of the spectrum is given by (e.g., see Kuik et al., 1998)

$$\theta_m = \arctan \left(\frac{\int_0^{2\pi} \int_{f_1}^{f_2} F(f, \theta) \sin \theta df d\theta}{\int_0^{2\pi} \int_{f_1}^{f_2} F(f, \theta) \cos \theta df d\theta} \right) \quad (\text{A6})$$

References

- Aarnes, O.J., Abdalla, S., Bidlot, J.R., Breivik, Ø., 2015. Marine wind and wave height trends at different ERA-interim forecast ranges. *J. Climate* 28, 819–837 <http://dx.doi.org/10.1175/JCLI-D-14-00470.1>.
- Alves, J.H., 2006. Numerical modeling of ocean swell contributions to the global wind-wave climate. *Ocean Modell.* 11, 98–122 <http://dx.doi.org/10.1016/j.ocemod.2004.11.007>.
- Ardhuin, F., Rogers, W.E., Babanin, A.V., Filipot, J., Magne, R., Roland, A., Van der Westhuysen, A., Queffeulou, P., Lefevre, J., Aouf, L., Collard, F., 2010. Semiempirical dissipation source functions for ocean waves. Part I: Definition, calibration, and validation. *J. Phys. Oceanogr.* 40, 1917–1941 <http://dx.doi.org/10.1175/2010JPO4324.1>.
- Babanin, A.V., 2011. *Breaking and Dissipation of Ocean Surface Waves*. Cambridge University Press 480 pp., ISBN: 9781107001589.
- Barber, N., Ursell, F., 1948. The generation and propagation of ocean waves and swell. I. Wave periods and velocities. *Philos. Trans. R. Soc. A* 240, 527–560 <http://rsta.royalsocietypublishing.org/content/240/824/527>.
- Barry, R., Chorley, R., 2009. *Atmosphere, Weather, and Climate*, 9th edition Routledge 536 pp., ISBN: 9780415465700.
- Benoit, M., Frigaard, P., Schäffer, H.A., 1997. Analysing multidirectional wave spectra: a tentative classification of available methods. In: Proc. Int. Association of Hydraulic Engineering and Research: Multidirectional Waves and Their Interaction with Structures. San Francisco, CA, pp. 131–157.
- Bidlot, J.R., Janssen, P.A.E.M., Abdalla, S., 2007. A revised formulation of ocean wave dissipation and its model impact. In: ECMWF Tech. Memo. 509. ECMWF, Reading, United Kingdom, Reading, United Kingdom 27 pp. http://old.ecmwf.int/publications/library/ecpublications/_pdf/tm/501-600/tm509.pdf.
- Boukhanovsky, A.V., Lopatoukhin, L.J., Guedes Soares, C., 2007. Spectral wave climate of the North Sea. *Appl. Ocean Res.* 29, 146–154 <http://dx.doi.org/10.1016/j.apor.2007.08.004>.
- Cavaleri, L., Alves, H., Ardhuin, F., Babanin, A., Banner, M., Belibassakis, K., Benoit, M., Donelan, M., Groeneweg, J., Herbers, T., Hwang, P., Janssen, P., Janssen, T., Lavrenov, I., Magne, R., Monbaliu, J., Onorato, M., Polnikov, V., Resio, D., Rogers, E., Sheremet, A., Smith, J., Tolman, H., Van Vledder, G., Wolf, J., Young, I., 2007. Wave modelling the state of the art. *Progr. Oceanogr.* 75 (4), 603e74 <http://dx.doi.org/10.1016/j.pocean.2007.05.005>.
- Chelton, D.B., Freilich, M.H., Esbensen, S.K., 2000. Satellite observations of the wind jets off the Pacific Coast of Central America. Part I: Case studies and statistical characteristics. *Mon. Wea. Rev.* 128, 1993–2018 [http://dx.doi.org/10.1175/1520-0493\(2000\)128<1993:SOOTWJ>2.0.CO;2](http://dx.doi.org/10.1175/1520-0493(2000)128<1993:SOOTWJ>2.0.CO;2).
- Chelton, D.B., Freilich, M.H., Esbensen, S.K., 2000. Satellite observations of the wind jets off the Pacific Coast of Central America, Part II: Regional relationships and dynamical considerations. *Mon. Wea. Rev.* 128, 2019–2043 [http://dx.doi.org/10.1175/1520-0493\(2000\)128<2019:SOOTWJ>2.0.CO;2](http://dx.doi.org/10.1175/1520-0493(2000)128<2019:SOOTWJ>2.0.CO;2).
- CIOH, Centro de Investigaciones Oceanográficas e Hidrográficas del Caribe, 2014. Sistema de Medición de Parámetros Oceanográficos y de Meteorología Marina (SMPOM). Online, last accessed 26/06/2014. <http://www.cioh.org.co/index.php/noticias-mainmenu-2-677/18-oceanografooperacional/519-sistema-de-medicion-parteos-oceanograficos-y-de-meteorologiamarina-smpom>.
- Collard, F., Ardhuin, F., Chapron, B., 2009. Monitoring and analysis of ocean swell fields from space: new methods for routine observations. *J. Geophys. Res.* V114, C07023 <http://dx.doi.org/10.1029/2008JC005215>.
- Deacon, G.E.R., 1949. Recent studies of waves and swell. *Ann. N. Y. Acad. Sci.* 51, 475–482.
- Dee, D., Uppala, S., Simmons, A., Berrisford, P., Poli, P., Kobayashi, S., et al., 2011. The ERA Interim reanalysis: configuration and performance of the data assimilation system. *Q. J. R. Meteorol. Soc.* 137, 553597 <http://dx.doi.org/10.1002/qj.828>.
- Donelan, M., Hamilton, J., Hui, W., 1985. Directional spectra of wind-generated waves. *Philos. Trans. R. Soc. Lond.* 315, 509–562.
- Drennan, W.M., Gruber, H.C., Hauser, D., Quentin, C., 2003. On the wave age dependence of wind stress over pure wind seas. *J. Geophys. Res.* 108, 8062 <http://dx.doi.org/10.1029/2000JC000715>.
- ECMWF, IFS. Documentation Cy36r1, 2011. Operational implementation 26 January 2010. PART VII: ECMWF WAVE MODEL. <http://old.ecmwf.int/research/ifsdocs/CY36r1/WAVES/IFSPart7.pdf>.
- EPRI (Electrical Power Research Institute), 2011. Mapping and Assessment of the United States Ocean Wave Energy Resource. 176 pp. <http://www1.eere.energy.gov/water/pdfs/mappingandassessment.pdf>.
- Hamilton, L.J., 2010. Characterising spectral sea wave conditions with statistical clustering of actual spectra. *Appl. Ocean Res.* 32 (3), 332–342 <http://dx.doi.org/10.1016/j.apor.2009.12.003>.
- Hasselmann, S., Bruning, C., Hasselmann, K., Heimbach, P., 1996. An improved algorithm for retrieval of ocean wave spectra from synthetic aperture radar image spectra. *J. Geophys. Res.* 101 (C7), 16615–16629.
- Holtzhausen, L.H., 2007. *Waves in Oceanic and Coastal Waters*. Cambridge University Press 404 pp., ISBN: 9780521129954.
- Janssen, P.A.E.M., 1991. Quasi-linear theory of wind-wave generation applied to wave forecasting. *J. Phys. Oceanogr.* 21, 1631–1642 [http://dx.doi.org/10.1175/1520-0485\(1991\)021<1631:QLTOWW>2.0.CO;2](http://dx.doi.org/10.1175/1520-0485(1991)021<1631:QLTOWW>2.0.CO;2).
- Janssen, P.A.E.M., 2004. *The Interaction of Ocean Waves and Wind*. Cambridge University Press 300 pp., ISBN: 9780521405403.
- Janssen, P.A.E.M., 2008. Progress in ocean wave forecasting. *J. Comput. Phys.* V227 (7), 3572–3594 <http://dx.doi.org/10.1016/j.jcp.2007.04.029>.
- Komen, G.J., Cavaleri, L., Donelan, M., Hasselmann, K., Hasselmann, S., Janssen, P., 1994. *Dynamics and Modelling of Ocean Waves*. Cambridge University Press 533 pp., ISBN: 9780521577816.
- Kuik, A.J., Van Vledder, G., Holtzhausen, L.H., 1988. A method for the routine analysis of pitch-and-roll buoy wave data. *J. Phys. Oceanogr.* 18, 1020–1034 [http://dx.doi.org/10.1175/1520-0485\(1988\)018<1020:AMFTRA>2.0.CO;2](http://dx.doi.org/10.1175/1520-0485(1988)018<1020:AMFTRA>2.0.CO;2).
- Longuet-Higgins, M.S., Cartwright, D.E., Smith, N.D., 1963. Observations of the directional spectrum of sea waves using the motion of a floating buoy. *Ocean Wave Spectra*. Prentice Hall, New York, pp. 111–136.
- Marineregions.org, 2014. Online, last accessed 26/06/2014, <http://www.marineregions.org>.
- Nwogu, O., 1989. Maximum entropy estimation of directional wave spectra from an array of wave probes. *Appl. Ocean Res.* 11, 176–182 http://www-personal.umich.edu/~onwogu/cv/nwogu_aor_1989.pdf.
- Ochi, M.K., 2005. *Ocean Waves: The Stochastic Approach*. Cambridge Ocean Technology Series. Cambridge University Press 332 pp., ISBN-13: 978-0521017671.
- Portilla, J., Ocampo-Torres, F., Monbaliu, J., 2009. Spectral partitioning and identification of wind sea and swell. *J. Atmos. Oceanic Technol.* 26, 107–122 <http://dx.doi.org/10.1175/2008JTECH0609.1>.
- Portilla, J., 2012. Storm-Source-Locating Algorithm Based on the Dispersive Nature of Ocean Swells. *Avances USFQ*, V4, C22–C36. http://www.usfq.edu.ec/publicaciones/avances/archivo_de_contenidos/Documents/volumen_4/Avances_2012_vol4_n1_C22-C36.pdf.
- Portilla, J., Caicedo, A., Padilla-Hernández, R., 2013. Observations of directional wave spectra in the Colombian Pacific. *Avances USFQ* V5, C5–C21 http://www.usfq.edu.ec/publicaciones/avances/archivo_de_contenidos/Documents/volumen_5_numero_2/c5_5_2_2013.pdf.
- Portilla, J., L. Cavalieri, G. Van Vledder, (submitted for publication). Wave spectra partitioning and long term statistical distribution. *J. Ocean Model.* <http://dx.doi.org/10.1016/j.ocemod.2015.06.008>.
- Raymond, D.J., Bretherton, C.S., Molinari, J., 2006. Dynamics of the intertropical convergence zone of the East Pacific. *J. Atmos. Sci.* 63, 582–597 <http://dx.doi.org/10.1175/JAS3642.1>.
- Schultz, D.M., Bracken, W.E., Bosart, L.F., 1998. Planetary- and synoptic-scale signatures associated with Central American cold surges. *Mon. Wea. Rev.* 126, 5–27 [http://dx.doi.org/10.1175/1520-0493\(1998\)126<0005:PASSA>2.0.CO;2](http://dx.doi.org/10.1175/1520-0493(1998)126<0005:PASSA>2.0.CO;2).
- Semedo, A., Weiss, R., Behrens, A., Sterl, A., Bengtsson, L., Günther, H., 2013. Projection of global wave climate change toward the end of the twenty-first century. *J. Climate* 26, 8269–8288 <http://dx.doi.org/10.1175/JCLI-D-12-00658.1>.
- Shih, H.H., 2003. Triaxys Directional Wave Buoy for Nearshore Wave Measurements – Test and Evaluation Plan, NOAA Technical Report NOS CO-OPS 38 Silver Spring, Maryland. <http://tidesandcurrents.noaa.gov/publications/tech rpt38.pdf>.
- Skey, S.G.P., Miles, M.D., 1999. Advances in buoy technology for wind/wave data collection and analysis, OCEANS '99 MTS/IEEE. Riding the Crest into the 21st Century 1, 113–118. doi: 10.1109/OCEANS.1999.799716, http://ieeexplore.ieee.org/xpl/freeabs_all.jsp?arnumber=799716&abstractAccess=no&userType=inst.
- Smith, W.H.F., Sandwell, D.T., 1997. Global seafloor topography from satellite altimetry and ship depth soundings. *Science* 277, 1956–1962 <http://www.sciencemag.org/content/vol277/issue5334>.
- Tavolato, C., Isaksen, L., 2011. Data usage and quality control in ERA-40, ERA-Interim, and the operational ECMWF data assimilation system. ECMWF, Reading, UK, ERA Report Series.
- Tolman, H.L., 2014. User manual and system documentation of WAVEWATCH III version 4.18. NOAA/NWS/NCEP/MMAB Technical Note 316, 194 pp. + Appendices.
- Tolman, H.L., Banner, M.L., Kaihatu, J.M., 2013. The NOPP operational wave model improvement project. *Ocean Modell.* 70, 2–10. doi: 10.1016/j.ocemod.2012.11.011.
- World Meteorological Organization, 1998. Provision and engineering/operational application of ocean wave data: UNESCO, Marine Meteorology and Related Oceanographic Activities Report No. 42, WMO/TD No 938, 347 pp.